การวัดความคลาดเคลื่อนของตำแหน่งการฉายรังสีในผู้ป่วยมะเร็งศีรษะและลำคอ ที่รักษาด้วย
เทคนิคฉายรังสีแบบปรับความเข้ม โดยใช้เครื่องถ่ายภาพทางรังสีแบบตัวเลข

นางสาวนันทพร นัยเนตร

วิทยานิพนธ์นี้เป็นส่วนหนึ่งของการศึกษาตามหลักสูตรปริญญาวิทยาศาสตรมหาบัณฑิต
สาขาวิชาฉายาเวชศาสตร์ ภาควิชารังสีวิทยา
คณะแพทยศาสตร์ จุฬาลงกรณ์มหาวิทยาลัย
ปีการศึกษา 2549
ลิขสิทธิ์ของจุฬาลงกรณ์มหาวิทยาลัย

MEASUREMENTS OF PATIENT'S SETUP VARIATION IN INTENSITY MODULATED RADIATION THERAPY OF HEAD AND NECK CANCER USING ELECTRONIC PORTAL IMAGING DEVICE

Miss Nantaporn Naiyanet

A Thesis Submitted in Partial Fulfillment of the Requirements
for the Degree of Master of Science Program in Medical Imaging
Department of Radiology
Faculty of Medicine
Chulalongkorn University
Academic Year 2006
Copyright of Chulalongkorn University

490649

Thesis Title   MEASUREMENTS OF PATIENT'S SETUP VARIATION IN INTENSITY MODULATED RADIATION THERAPY OF HEAD AND NECK CANCER USING ELECTRONIC PORTAL IMAGING DEVICE

By   Miss Nantaporn Naiyanet

Field of Study   Medical Imaging

Thesis Advisor   Assistant Professor Chawalit Lertbutsayanukul, M.D.

Thesis Co-advisor   Associate Professor Sivalee Suriyapee, M.Eng.

Accepted by the Faculty of Medicine, Chulalongkorn University in Partial Fulfillment of the Requirements for the Master's Degree

…………………………….Dean of the Faculty of Medicine
(Professor Pirom Kamol-ratanakul, M.D., M.Sc.)

THESIS COMMITTEE:

…………………………………………….Chairman
(Associate Professor Somjai Wangsuphachart, M.D.)

……………………………………………Thesis Advisor
(Assistant Professor Chawalit Lertbutsayanukul, M.D.)

…………………………………..Thesis Co-advisor
(Associate Professor Sivalee Suriyapee, M.Eng.)

………………………………………………...Member
(Assistant Professor Chumpot Kakanaporn, M.Sc.)

………………………………………………...Member
(Mrs. Weeranuch Kitsukjit, M.Sc.)

นันทพร นัยเนตร : การวัดความคลาดเคลื่อนของตำแหน่งการฉายรังสีในผู้ป่วยมะเร็งศีรษะและลำคอ ที่รักษา ด้วยเทคนิคฉายรังสีแบบปรับความเข้ม โดยใช้เครื่องถ่ายภาพทางรังสีแบบตัวเลข. (MEASUREMENTS OF PATIENT'S SETUP VARIATION IN INTENSITY MODULATED RADIATION THERAPY OF HEAD AND NECK CANCER USING ELECTRONIC PORTAL IMAGING DEVICE). อ.ที่ปรึกษา: ผศ.นพ. ชวลิต เลิศบุษยานุกูล, อ.ที่ปรึกษาร่วม: รศ. ศิวลี สุริยาปี; 71 หน้า.

การรักษาผู้ป่วยมะเร็งศีรษะและลำคอด้วยเทคนิคฉายรังสีแบบปรับความเข้มนั้น เป็นเทคนิคที่ให้ลำรังสีคลุม เฉพาะขอบเขตของก้อนมะเร็งและหลีกเลี่ยงปริมาณรังสีที่อวัยวะใกล้เคียง แพทย์ได้ทำการฉายรังสีที่เผื่อขอบเขตออกไป เล็กน้อย เพื่อป้องกันความคลาดเคลื่อนที่อาจเกิดขึ้นได้จากการจัดท่าผู้ป่วย ดังนั้นการฉายรังสีจึงจำเป็นที่จะต้องถูกต้อง คงที่และแม่นยำ อย่างไรก็ตามในระหว่างการฉายรังสีแต่ละครั้งนั้นอาจเกิดความคลาดเคลื่อนขึ้นได้ซึ่งอาจเกิดมาจากระบบ หรืออาจเกิดแบบสุ่ม โดยความคลาดเคลื่อนจากระบบนั้นเกิดเมื่อมีความแตกต่างของตำแหน่งขณะฉายรังสีจริงกับตำแหน่ง จากการวางแผนการรักษา ความคลาดเคลื่อนเฉลี่ยนี้เรียกว่าความคลาดเคลื่อนจากระบบ และความคลาดเคลื่อนของ ตำแหน่งในการฉายรังสีแต่ละครั้งนั้นเรียกว่า ความคลาดเคลื่อนแบบสุ่ม

การศึกษาวิจัยในครั้งนี้ มีวัตถุประสงค์เพื่อ วัดความคลาดเคลื่อนของตำแหน่งการฉายรังสีในผู้ป่วยมะเร็งศีรษะ และลำคอ ที่รักษาด้วยเทคนิคฉายรังสีแบบปรับความเข้มที่มีการเคลื่อนที่ของลำรังสี เพื่อดูว่าขอบเขตที่เผื่อไว้เดิมเหมาะสม หรือจะต้องปรับเปลี่ยนโดยทำการศึกษาในผู้ป่วยมะเร็งศีรษะและลำคอจำนวน 9 ราย ในช่วงเดือนมีนาคมถึงเดือน พฤศจิกายน 2549 ที่มารักษาด้วยเทคนิคฉายรังสีแบบปรับความเข้ม โดยใช้รังสีเอ็กซ์ขนาด 6 เมกะโวลต์จากเครื่องเร่ง อนุภาค Varian Clinac 23EX ซึ่งมีเครื่องถ่ายภาพรังสีแบบตัวเลขสำหรับถ่ายภาพตรวจสอบตำแหน่งการฉายรังสี

ในการวิจัยนี้ศึกษาโดยการนำภาพถ่ายก่อนการฉายรังสีทุกๆสัปดาห์ มาเปรียบเทียบกับภาพที่ได้จากการจำลอง การรักษาซึ่งใช้เป็นภาพอ้างอิงโดยเลือกใช้ตำแหน่งอ้างอิง 6 ตำแหน่ง โดยถ่ายภาพตำแหน่งการฉายรังสี 3 ภาพได้แก่ ด้านหน้าและด้านข้าง และภาพถ่ายตำแหน่งการฉายรังสีด้านหน้าระดับไหล่ ในทุกๆสัปดาห์ เพื่อหาความคลาดเคลื่อนของ ตำแหน่งการฉายรังสี ด้วย ซอฟต์แวร์ VARiS Vision วัดค่าความคลาดเคลื่อนในแนว X (ซ้าย-ขวา), Y (บน-ล่าง) สำหรับ ภาพถ่ายตำแหน่งการฉายรังสีด้านหน้า และ ในแนว Z (หน้า-หลัง), Y (บน-ล่าง) สำหรับภาพถ่ายตำแหน่งการฉายรังสี ด้านข้าง

จากผลการวิเคราะห์ภาพทั้งหมด 168 ภาพ ซึ่งได้แก่ภาพที่ได้จากการจำลองการรักษา 27 ภาพและภาพถ่ายก่อน การฉายรังสี 141 ภาพ พบว่าความคลาดเคลื่อนจากระบบในผู้ป่วยแต่ละรายอยู่ในช่วง 0 ถึง 7.5 มิลลิเมตร ในขณะที่ความ คลาดเคลื่อนแบบสุ่มในผู้ป่วยแต่ละรายอยู่ในช่วง 0.3 ถึง 4.8 มิลลิเมตร เมื่อนำค่าความคลาดเคลื่อนมาคำณวนหาขอบเขต การฉายรังสีที่เหมาะสม สำหรับภาพถ่ายตำแหน่งการฉายรังสีด้านหน้าพบว่าอยู่ในช่วง 2.4 ถึง 4.9 มิลลิเมตร และ 3.9 ถึง 5.0 มิลลิเมตร ในแนวซ้าย-ขวา และ บน-ล่าง ตามลำดับ ในขณะที่ขอบเขตการฉายรังสีที่เหมาะสมสำหรับภาพถ่าย ตำแหน่งการฉายรังสีด้านข้างอยู่ในช่วง 3.4 ถึง 4.7 มิลลิเมตร และ 2.6 ถึง 3.7 มิลลิเมตร ในแนวหน้า-หลังและ บน-ล่าง ตามลำดับ ความแตกต่างในแนวบน-ล่าง ระหว่างภาพด้านหน้าและด้านข้างเนื่องมาจากกระดูกไหปลาร้าที่ใช้เลือกเป็น ตำแหน่งอ้างอิงในภาพด้านหน้านั้นมีความคงที่น้อยกว่าอวัยวะที่ใช้เลือกเป็นตำแหน่งอ้างอิงในภาพด้านข้าง เมื่อนำ ขอบเขตการฉายรังสีที่เหมาะสมที่คำณวนได้เปรียบเทียบกับขอบเขตการฉายรังสีที่ใช้โรงพยาบาลจุฬาลงกรณ์ใช้อยู่ใน ปัจจุบันคือ 5 ถึง 10 มิลลิเมตร พบว่าขอบเขตการฉายรังสีที่คำณวนได้น้อยกว่าหรือเท่ากับ 5 มิลลิเมตร จากผลการศึกษา แสดงให้เห็นว่าการขยายขอบเขตที่ใช้อยู่ในปัจจุบันนั้นครอบคลุมผู้ป่วยมะเร็งศีรษะและลำคอทั้งหมดที่รักษาด้วยเทคนิค ฉายรังสีแบบปรับความเข้ม

ภาควิชา	รังสีวิทยา	ลายมือชื่อนิสิต	นันทพร นัยเนตร
สาขาวิชา	ฉายาเวชศาสตร์	ลายมือชื่ออาจารย์ที่ปรึกษา	ชวลิต เลิศบุษยานุกูล
ปีการศึกษา	2549	ลายมือชื่ออาจารย์ที่ปรึกษาร่วม	ศิวลี สุริยาปี

4874743730: MAJOR MEDICAL IMAGING

KEYWORDS: ELECTRONIC PORTAL IMAGING /INTENSITY MODULATED RADIATION THERAPY / CTV-TO-PTV MARGIN / HEAD AND NECK CANCER.

NANTAPORN NAIYANET: MEASUREMENTS OF PATIENT'S SETUP VARIATION IN INTENSITY MODULATED RADIATION THERAPY OF HEAD AND NECK CANCER USING ELECTRONIC PORTAL IMAGING DEVICE. THESIS ADVISOR: ASST. PROF. CHAWALIT LERTBUTSAYANUKUL, CO-ADVISOR: ASSOC. PROF. SIVALEE SURIYAPEE, 71 pp.

The introduction of IMRT poses new challenges for delivering intended target dose and minimizing dose and toxicity to critical normal structures. For head and neck cancer, reproducible patient positioning throughout the whole treatment course is particularly important due to the proximity of many critical organs. Deviations from the planned irradiation geometry during a treatment session may be systematic or random. Systematic errors occur if the mean irradiation geometry in the fractionated treatment differs from the geometry in the treatment plan. The mean deviations are then called systematic errors. Fraction-to-fraction variations around the mean deviation are called random errors.

The purpose of this study is to measure the interfraction setup variation of patient undergoing IMRT of head and neck cancer. The data is used to define adequate treatment clinical target volume to planning target volume (CTV-to-PTV) margin. During March to November 2006, the data was collected from 9 head and neck cancer patients treated with dynamic IMRT using 6 MV X-ray beam from Varian Clinac 23EX. Weekly portal images of setup fields which were anterior-posterior and lateral portal images were acquired for each patient with an amorphous silicon EPID, Varian aS500. These images were matched with the reference images from Varian Acuity simulator using the VARiS Vision software, version 7.3.10. Six anatomical landmarks were selected for comparison. The displacement of portal image from the reference image was recorded in X (Left-Right, L-R), Y (Superior-Inferior, S-I) direction for anterior field and Z (Anterior-Posterior, A-P), Y (S-I) direction for lateral field. The systematic and random error for individual and population were calculated. Then the population-based margins were obtained. The total of 168 images (27 simulation images and 141 portal images) and 564 match points were evaluated. The results showed that the systematic error ranged from 0 to 7.5 mm and the random error ranged from 0.3 to 4.8 mm for all direction. The population-based margin ranged from 2.4 to 4.9 mm (L-R), 3.9 to 5.0 mm (S-I) for anterior field and 3.4 to 4.7 mm (A-P), 2.6 to 3.7 mm (S-I) for the lateral field. The difference in population-based margins along S-I axis between anterior field and lateral field were observed because the clavicles chosen for anterior field at the shoulder level were less stable than anatomical landmarks chosen for lateral field i.e. skull bones, C1 and C4. These margins were comparable to the margin that prescribed at King Chulalongkorn Memorial Hospital (5 - 10 mm) for head and neck cancer. These results showed that the population-based margin is less than 5mm, thus the margin provides sufficient coverage for all of the patients.

Department	Radiology	Student's signature	Nantaporn Naiyanet
Field of study	Medical Imaging	Advisor's signature	Chawalit Lertbutsayanukul
Academic year	2006	Co-advisor's signature	Sivalee Suriyapee

ACKNOWLEDGEMENTS

CONTENTS

LIST OF TABLES

Table   **Page**

LIST OF FIGURES

Figure   **Page**

Figure   **Page**

LIST OF ABBREVIATIONS

Abbreviation	Terms
3-D CRT	Three dimensional conformal radiation therapy
A-P	Anterio-Posterior
a-Si, aSi	Amorphous silicon
C-C	Cranio-Caudal
cGy	Centigray
cm	Centimeter
cm^2	Square centimeter
cm^3	Cubic centimeter
C1	First cervical vertebral body
C4	Fourth cervical vertebral body
CT	Computed Tomography
CRF	Case Record Form
CTV	Clinical target volume
DART	Dynamic Adaptive Radiation Therapy
DICOM	Digital imaging and communications in medicine
DMLC	Dynamic multileaf collimator
DRRs	Digitally reconstructed radiographs
DVHs	Dose volume histrograms
EPID	Electronic portal imaging device
FP	Fixation points
GTVs	Gross tumor volumes

Abbreviation	Terms
Gy	Gray
IM	Internal margin
ICRU	International Commission on Radiation Units and Measurements
IGRT	Image Guided Radiation Therapy
IMRT	Intensity modulated radiation therapy
ITV	Internal target volume
ISO	International standard organization
L-R	Left-Right
MU	Monitor unit
MV	Megavoltage
MLC	Multileaf collimator
MRI	Magnetic resonance imaging
mg	Milligram
min	Minute
M-L	Medio-Lateral
mm	Millimeter
NTD	Normalized total dose
OAR	Organ at risk
PET	Positron emission tomography
PID	Portal Imaging Device
PMMA	Polymethylmethacrylate
PRVs	Planning organ at risk volumes

Abbreviation	Terms
PTVs	Planning target volumes
QA	Quality assurance
RL	Right lateral
SD	Standard deviation
S-I	Superior-Inferior
SMLC	Static multileaf collimator
s	Second
TPS	Treatment planning system
Σ	Systematic error
Σ_{ind}	Individual systematic error
Σ_{pop}	Population systematic error
σ	Random error
σ_{ind}	Individual random error
σ_{pop}	Population random error

CHAPTER 1

INTRODUCTION

1.1 Background and Rationale

Radiotherapy for head and neck cancer requires accuracy of radiation dose to the target volume. Reproducing of the patient setup in the head and neck area is particularly important due to the proximity of many critical organs (eye, optic chiasm, brain stem, spinal cord and so on). The introduction of new technology such as intensity modulated radiation therapy (IMRT) and 3D conformal radiation therapy (3D CRT) poses new challenges for delivering intended target dose and minimizing dose and toxicity to critical normal structures. This is accomplished by conforming the treatment fields to the target volume, using appropriate margins to account for treatment uncertainties. To determine these margins between the clinical target volume (CTV) and field borders, the concept of the planning target volume (PTV) has been introduced by International Commission on Radiation Units and Measurement (ICRU) [1]. The planning target volume (PTV) is the CTV plus a margin to allow for geometrical uncertainty in its shape and variations in its location relative to the radiation beams due to organ mobility, organ deformation, and patient setup variations. Intermittent monitoring of the setup accuracy is prudent and may lead to discovery of errors that could otherwise go undetected. Assessing the accuracy of patient/beam alignment or the effectiveness of an immobilization device is important and the result should be considered when field margins are designed. Thus, if port films are consistently inadequate, an increase the field margins or an improvement of the immobilization might be indicated. The most common methods to monitor treatment accuracy are visual comparison of simulation film (prescription) and port film (treated) or electronic portal imaging. This traditional method suffers from deficiencies that some setup errors go undetected and others persist for a clinically significant portion of the prescribed dose. For example, a field shaping block, omitted or inserted in the wrong orientation during a treatment delivered between port-filming days, would not be detected. Likewise, misinterpretation of setup marks leading to setup errors could be undetected for several days. Significant improvements in both accuracy and efficiency of detecting and correcting setup errors can, in principle, be achieved by using electronic portal imaging devices where the setup is verified prior to each treatment and, in some situations, also during the treatment. Setup errors can be measured using portal imaging by apply megavoltage film or an electronic portal imaging device (EPID). Megavoltage film measurements are rather time consuming and not always very accurate. Since 2005, EPIDs have become available in Division of Radiation Oncology, King Chulalongkorn Memorial Hospital, to check the setup accuracy.

At present, a CTV-to-PTV margin ranging from 5 mm to 10 mm is prescribed to patient undergoing IMRT of head and neck cancer at our division. However, a too small CTV-to-PTV margin may result in geometrical miss at some or even all treatment fractions. It, therefore, becomes increasingly important to define adequate CTV-to-PTV margin. RTOG protocol H-0022 [2], suggests using a uniform CTV-to-PTV margin of at least 5 mm until the institution specific uncertainty has been evaluated. To improve the confidence in patient-specific margin, therefore, the purpose of this study is to extract quantitative data from direct measurements of

interfraction setup variation in head-and-neck patients undergoing IMRT. The data will be used to define adequate CTV-to-PTV margin.

1.2 Objective

1.2.1 To extract quantitative data from direct measurements of interfraction setup variation of patient undergoing IMRT of head and neck cancer.

1.2.2 To define adequate CTV-to-PTV margin.

CHAPTER 2

REVIEW OF RELATED LITERATURE

2.1 Theory

2.1.1 Head-and-Neck Cancer [3]

Head-and-neck cancer is the term given to a variety of malignant tumors that develop in the oral cavity (mouth); pharynx (throat); paranasal sinuses (small hollow spaces around the nose lined with cells that secrete mucus); nasal cavity (airway just behind the nose); larynx ("Adam's apple" or voice box); and salivary glands (parotid, submanidular, sublingual glands that secrete saliva). Many authorities also include skin tumors of the face and neck and tumors of the cervical lymph nodes. Nasopharyngeal cancer is the most common head-and-neck cancer in Thailand. The incidence of nasopharyngeal cancer is highest in both males and females in Bangkok with age-standardized rate of 4.5 per 100000 male populations and 1.6 per 100000 female populations [4].

2.1.1.1 Risk Factors

Factors known to contribute to the risk of developing head and neck cancers include smoking (both tobacco and marijuana) or chewing tobacco and frequent alcohol use. Leukoplakia (white spots or patches in the mouth) also may be considered a risk factor, as this condition becomes cancerous in approximately one-third of patients.

2.1.1.2 Pathology

Most head-and-neck cancers are squamous cell carcinomas, tumors that develop in the tissue lining the hollow organs of the body. However, other tumor types also may be seen and include lymphoepithelioma, spindle cell carcinoma, verrucous cancer, undifferentiated carcinoma and cancers of the lymph nodes, called lymphoma (most often diffuse non-Hodgkins lymphoma).

2.1.1.3 Signs and Symptoms

Cancers of the head-and-neck are some of the few cancers for which a particular cause can often be identified. When examined, patients who report the symptoms described below commonly admit to being smokers and/or frequent consumers of substantial quantities of alcohol. In fact, some doctors candidly admit that it is quite rare to see patients with head and neck cancer who do not smoke or drink excessively. The common symptoms of cancer of the head and neck include persistent pain in the throat; pain or difficulty with swallowing; persistent hoarseness or a change in voice; pain in the ear; and bleeding in the mouth or throat. Because about half of all head and neck cancers originate in the oral cavity, sores or lesions in the mouth can be warning signs. Two types of lesions that could be precursors to cancer are leukoplakia (white lesions) and erythroplakia (red lesions). Although less common than leukoplakia, erythroplakias have a much greater potential for becoming

cancerous. Any white or red lesion that does not heal or disappear in 2 weeks should be evaluated by a physician and considered for biopsy. Anyone experiencing such symptoms for more than 2 weeks should see their physician as soon as possible for a thorough examination and laboratory tests. If a diagnosis cannot be obtained, your physician will refer you to a specialist.

2.1.1.4 Diagnosis

Establishing a diagnosis for head and neck cancers typically begins with an examination and biopsy of any identified suspected cancerous lesions or tumors. This involves extracting a piece of suspicious tissue and sending it to a laboratory for examination. In some cases the biopsy can be performed in the physician's office, although it is more common for the procedure to be done in an operating room under anesthesia.

2.1.1.5 Staging

Staging is the process of describing the extent to which cancer has spread from the site of its origin. It is used to assess a patient's prognosis and to determine the choice of therapy. The stage of a cancer is determined by the size and location in the body of the primary tumor, and whether it has spread to other areas of the body.

Staging involves using the letters T, N and M to assess tumors by: the size of the primary tumor (T); the degree to which regional lymph nodes (N) are involved. Lymph nodes are small organs located along the channels of the body's lymphatic system which store special cells that fight infection and other diseases); and the absence or presence of distant metastases (M) - cancer that has spread from the original (primary) tumor to distant organs or distant lymph nodes.

Each of these categories is further classified with a number 1 through 4 to give the total stage. Thus a T1-N1-M0 cancer would describe a T1 tumor, N1 lymph node involvement, and no metastases. Once the T, N and M are determined, a "stage" of I, II, III or IV is assigned:

Stage I cancers are small, localized and usually curable.

Stage II and III cancers typically are locally advanced and/or spread to local lymph nodes.

Stage IV cancers usually are metastatic (spread to distant parts of the body) and generally are considered inoperable.

The staging system for head and neck cancers is a bit complicated. Though the nodal and metastasis staging systems are the same for all the different anatomical regions of the head and neck, the tumor staging systems are different.

2.1.1.6 Treatment and Clinical Trials

Head-and-neck cancer is often complex, with many different sites and staging systems. However, current therapy offers several alternatives, including surgery, radiation, and chemotherapy, either alone or in combination. Combined modality therapy is becoming the principal method of treating patients with locally advanced head and neck cancers. Radiation may cause difficulty swallowing, mouth sores, and skin reactions (e.g., redness, itching, burning). Patients also may want to explore the possibility of participating in a clinical trial. Clinical trials may offer cutting-edge therapy and also provide oncologists, surgeons, and radiation oncologists the

opportunity to further refine and improve treatment options. Physician can determine if a patient is eligible for a clinical trial.

2.1.2 Intensity Modulated Radiation Therapy (IMRT) for Head-and-Neck Cancer [5, 6]

Intensity-modulated radiation therapy (IMRT) is a state-of-the-art cancer treatment method that can delivers high doses of radiation directly to cancer cells in a very targeted way, much more precisely than is possible with conventional radiotherapy. IMRT can deliver higher radiation doses directly to cancer cells while sparing more of the surrounding healthy tissue. This has important advantages in oral cancers as it allows the beams to hit their target area while missing the surrounding structures such as the salivary glands.

IMRT is an advanced form of three-dimensional conformal therapy (3DCRT). Unlike conventional conformal therapy, the beam intensity of each IMRT field is modulated in a rather complex way. Delivery of intensity-modulated fields relies on the use of computer controlled multileaf collimators (MLCs) equipped on modern linear accelerators. Because of the complex beam intensity modulation, each IMRT field often includes many small, irregular, off-axis fields resulting in isodose distributions for each IMRT plan that are more conformal to the tumor target volume than those from conventional treatment plans.

2.1.2.1 Procedure of IMRT Treatment [5]

Similar to conventional conformal therapy, processes of IMRT treatment include treatment setup, patient immobilization, computed tomography (CT) image acquisition, treatment planning, treatment verification, and the actual treatment. A flow chart for an IMRT procedure is shown in Figure 2.1.
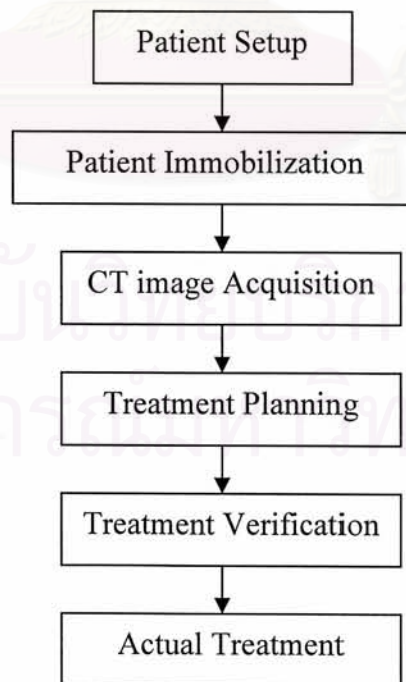
Figure 2.1 An IMRT procedure flow chart.

The anatomy of the neck is complex, with many critical and radiation-sensitive organs in close proximity to the targets. Tight dose gradients around the targets that limit the doses to the noninvolved tissue, features characteristic of IMRT, are desirable and offer the potential for therapeutic gains. Noninvolved tissues whose sparing may offer tangible gains include the major salivary glands, the minor salivary glands dispersed within the oral cavity, and the mandible. In cases of nasopharyngeal and paranasal sinus cancer, critical normal tissue that may be partly spared using IMRT includes the inner and middle ears, temporomandibular joints, temporal lobe of the brain, and optic pathways. In addition to noninvolved tissue sparing, IMRT offers the potential for improved tumor control by reducing the constraints on the tumor dose owing to critical organs (eg, the spinal cord, brainstem, and optic pathways) that may limit the tumor boost doses in conventional RT. This is achieved by specifying a maximum dose to the critical organs and a high penalty in the optimization process if that dose is exceeded. In addition, IMRT eliminates the need for posterior neck electron fields, which are commonly used in conventional RT, and their associated dose deficiencies. IMRT in the head and neck is more feasible than in other sites because organ motion is practically absent. The only factor that has to be taken into account is patient setup uncertainties. This can be addressed by using adequate immobilization and by assessing the resulting setup variations.

2.1.2.2 Patient Selection [6]

Head and neck IMRT is labor intensive and lengthens treatment time. Not every patient is expected to benefit. Those who would benefit the most are patients with paranasal sinus or advanced nasopharyngeal cancer in whom the targets are near the optic pathways, patients with oropharyngeal or nasopharyngeal cancer in whom standard RT fields would encompass most of the salivary glands, and, similarly, patients with laryngeal cancer who present with advanced nodal disease. In many patients with locally advanced head-and-neck tumors, standard techniques would require a compromise in the tumor dose owing to the proximity of the tumor to the spinal cord or to the brainstem. In these cases, the advantage of IMRT, through its ability to produce concave dose distributions, is obvious. The isodose distributions of an IMRT plan is shown in Figure 2.2. Patients with laryngeal cancer and clinically noninvolved cervical lymph nodes receiving treatment to the larynx alone or requiring irradiation of the neck encompassing the jugulodigastric nodes but not extending to the base of the skull may not benefit from IMRT compared with simpler techniques. The same applies to patients requiring irradiation to the ipsilateral neck alone. Additional concerns relate to the doses delivered to the oral cavity in cases of oral cavity or oropharyngeal cancer, in which IMRT may have an advantage over standard RT in partial sparing of the oral cavity, especially where the primary tumor is lateralized. Such sparing is expected to reduce the extent of acute mucositis and improve longterm xerostomia through the reduction in the volume of the minor salivary glands exposed to high radiation doses.

2.1.2.3 Immobilization [6]

Head and neck immobilization is typically performed using a thermoplastic mask with several attachment points to the treatment table and a head support. Several commercial systems are available. Typically, immobilization with these systems results in daily setup errors of a few millimeters. These errors require an extension of the targets by 3 to 5 mm to ensure adequate irradiation. If the targets in the lower neck and the supraclavicular nodes are included in the IMRT plans, it is important to extend the mask to include the lower neck and shoulders, such that the lower neck is immobilized. This may enhance skin reactions in the low-lateral neck owing to a bolus effect of the mask, which increases the dose to the skin delivered by beams, which are tangential to the skin. Cutting holes in the low-lateral parts of the mask, bilaterally, reduces the skin effects remarkably as shown in Figure 2.3. An alternative used in many institutions is to treat the lower neck with an anterior field. This field matches to the IMRT fields treating the primary tumor and the upper neck using a split-beam technique. In these cases, the head and upper neck alone need to be immobilized. Skin effects are expected to be less severe using this method, and the time required for target delineation is reduced. However, in these cases, the targets in the low neck are not expected to receive the full prescribed doses. This approach is justified when the risk of subclinical disease in the low neck is small, such as in patients with no or minimal clinical evidence of upper neck disease.
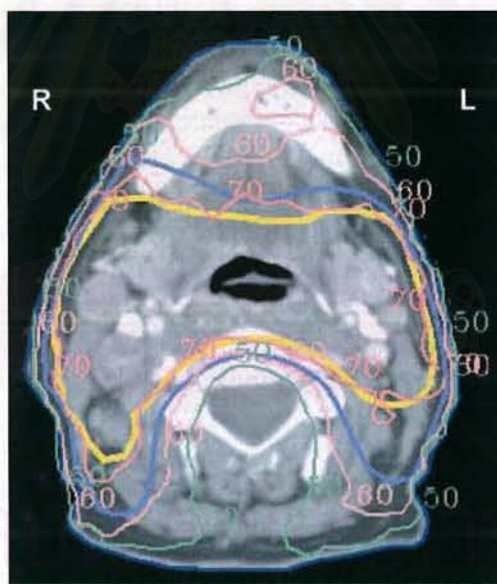
Figure 2.2 Isodose distributions of an intensity-modulated radiation therapy plan for posterior pharyngeal wall cancer. The concave shapes of the planning target volumes (PTVs) of the tumor and lymph node metastases (yellow) and the PTV of subclinical disease (blue) are well covered by the prescribed isodoses (70 and 60 Gy, respectively).

Figure 2.3 Immobilization of both neck and shoulders is necessary if the targets in the low neck are included in the intensity-modulated radiation therapy plans. Cutting holes in the mask in the low neck, bilaterally, reduces skin reactions.

2.1.2.4 Target Selection and Delineation [6]

A major potential pitfall of IMRT is the failure to select and delineate the targets accurately. This is especially relevant in head and neck cancer, in which a high risk of subclinical local and nodal disease exists and adequate irradiation of the lymph nodes at risk is crucial for local-regional control and survival. For example, in standard three-field RT of oropharyngeal cancer, the first echelon and the retropharyngeal nodes are treated when the primary tumor is targeted. In contrast, these nodes will not be adequately irradiated by IMRT if they are not specified as targets on the planning CT. The gross tumor volumes (GTVs) consist of the primary tumor and of lymph nodes with apparent or suspected metastasis. Lymph node GTVs include nodes with radiologic criteria of involvement: diameter > 1 cm (in the case of the jugulodigastric nodes, > 1.1–1.5 cm), smaller nodes with spherical rather than ellipsoid shape, nodes containing inhomogeneities suggestive of necrotic centers, or a cluster of three or more borderline nodes, or PET-positive nodes. The clinical target volume (CTV) surrounding the primary tumor consists of tissue perceived to contain a microscopic, subclinical tumor extension. In addition to the primary tumor CTV, the lymphatic CTVs consist of nodal areas that are at risk of metastatic disease but do not match the radiologic criteria of involved nodes.

2.1.2.5 Planning Target Volumes [6]

After the GTVs and the CTVs are delineated on the axial CT images, a uniform expansion of these targets is performed to obtain the planning target volumes (PTVs) that accommodate setup uncertainties (typically by 3–5 mm). Doses are prescribed to the PTVs or to comparable "growth" areas in some commercial planning systems. When the targets are close to the skin, as may occur in postoperative cases, the PTV may extend beyond the surface. In such cases, the PTV should be "edited" back to the surface. If the PTV extends to the skin, but the skin is not at high risk, the external body contour may be defined as a noninvolved organ for the optimization system. This may facilitate avoiding excessive dosing to the skin. Similar to the

expansion of the targets to yield the PTVs, there is a need to accommodate uncertainties regarding the critical normal organs, especially the spinal cord, brainstem, and optic pathways, that may lie in regions of steep dose falloff near the targets. This can be accomplished by expanding these organs uniformly, yielding the planning risk volumes (PRVs). Similarly, the optic nerves and chiasm are expanded by 3 to 5 mm for treatment plans of nasopharynx or paranasal sinus tumors. No margins are usually given to accommodate potential organ motion in head and neck IMRT. In a study of intrafraction motion of the larynx during RT, it was found that the incidence and duration of swallowing were very low; therefore, they need not be taken into account. However, the tip of the epiglottis was found to move within a range of 7 mm. This may have implications for the expansion of the primary target in cases of supraglottic larynx cancer.

2.1.2.6 Prescription and Normal Tissue Dose Constraints [6]

The delivery of a single treatment plan throughout the course of treatment provides better dose conformity compared with several consecutive plans and is therefore typical of IMRT. This deviates substantially from the practice of standard RT for head and neck cancer. When a single plan is prescribed, the gross tumor PTV receives both a higher total dose and a higher dose per fraction than the PTVs representing subclinical disease. Owing to the differences in the daily fraction doses, a correction of the total dose to yield the normalized total dose (NTD) for a 2 Gy fraction regimen is required when the fraction dose is substantially different from standard fractionation. Dose prescription modes for head and neck IMRT can be divided into two general approaches. The first would be the prescription of total dose and treatment duration that deliver a standard fraction dose of 2 Gy to the gross disease PTV, for example, 70 Gy over 35 fractions, whereas lower than standard fraction doses are prescribed to the subclinical disease PTVs. When used for advanced disease, this schedule should be delivered concurrently with chemotherapy. This approach is used at the University of Michigan for stage III to IV head and neck cancer, and the chemotherapy agents delivered concurrently with IMRT consist of combinations of cisplatin or carboplatin and paclitaxel. The second strategy is to deliver a higher-than-standard fraction dose to the gross disease PTV, adjusting the total dose to yield NTD near 70 Gy, and standard fraction doses to the elective target PTVs. Such a strategy was adopted by the RTOG study of IMRT for oropharyngeal cancer [2].

2.1.2.7 Beam Number and Orientation [6]

IMRT using MLCs requires one to choose the number and orientation of the treatment beams. It was suggested early on that if the number of segments (or beamlets) is large enough, the direction of the beams is not important, and coplanar beams arranged at equidistance around the patient's head and neck would achieve satisfactory results. Most investigations of IMRT of the head and neck with MLCs use this approach. The beam number should be odd to prevent opposed beams, which would increase hot spots near their entrance to the neck. Nine beams arranged at equidistance (40° apart) were found to be optimal; they provided better dose distributions than five or seven beams, whereas 15 beams did not seem to improve the plans. Optimization of the beam angles was found to be unnecessary by some authors, whereas others reported an improvement in head and neck plans when optimized,

noncoplanar beam angles were used. This issue continues to be a subject to research, whereas the current recommended field arrangement for IMRT of head and neck cancer with MLCs is nine equidistant coplanar fields as shown in Figure 2.4. At the King Chulalongkorn Memorial hospital, complex cases such as nasopharyngeal cancer or advanced tumors in other sites, or cases with clinical evidence of bilateral neck disease, are planned using nine equidistant beams. In less advanced cases in which the neck requires treatment bilaterally, five or seven equidistant beams may achieve satisfactory results. Choosing the lowest number of beams that achieves the planning objectives is expected to reduce treatment time and increase efficiency.
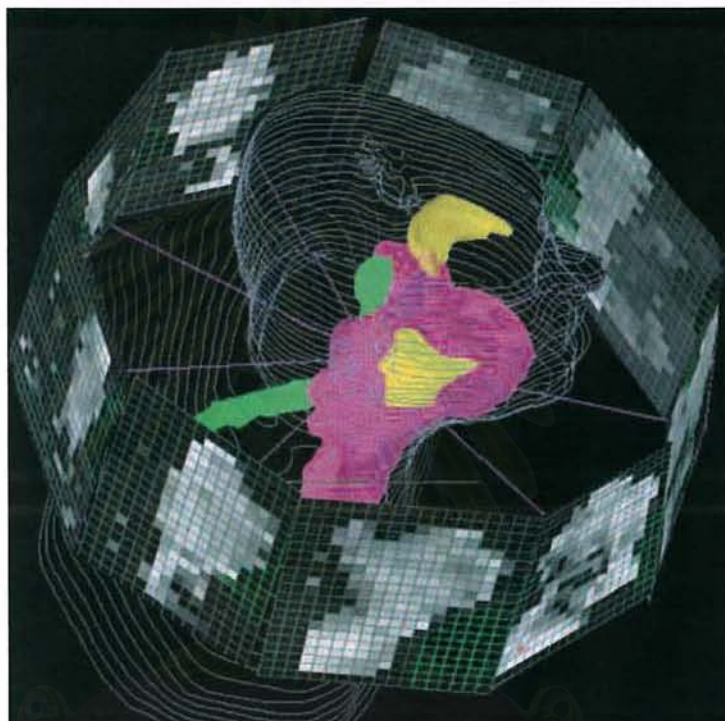
Figure 2.4 Using a multileaf collimator, nine equidistant coplanar beams are recommended for advanced cases.

2.1.3 Target and Critical Structure Definitions [7]

The safe and effective implementation of IMRT invites a well-prepared radiotherapy department to re-visit the overall process of treatment planning. While the general concepts are comparable to those necessary for forward-planned, three-dimensional (3-D) conformal radiotherapy, the presence of steeper dose gradients, possible tighter margins, and differences in delivery techniques require further thought about all steps to be considered in developing and implementing a treatment plan.

2.1.3.1 ICRU Report 50 and ICRU Report 62 [1]

To help ensure accuracy and consistency in dose prescriptions, the ICRU has recommended a convention for dose reporting. The original form of these recommendations for external beam radiotherapy was ICRU report 50 (ICRU 50, 1993). The key concepts presented in ICRU report 50 are illustrated in Figure 2.5. The gross tumor volume (GTV) indicates the physician's observation of the tumor based on the imaging data available. In order to account for the likelihood of clonogenic tumor outside of the visualized GTV boundary, the clinical target volume (CTV), an expansion of the GTV, is created. The further uncertainty in tumor location due to setup error and/or internal organ movement and anatomic changes are considered in the planning target volume (PTV), and expansion of the CTV. Significant research has been applied recently in order to estimate necessary PTV expansions for different body regions. While the constructs presented in ICRU report 50 provide the potential for ensuring adequate dose to tumor in most instances, there are a few limitations for treatment planning that remain to be addressed. ICRU report 62 (ICRU 62, 1999) deals with some of these issues. The additional constructs are described in Figure 2.6.
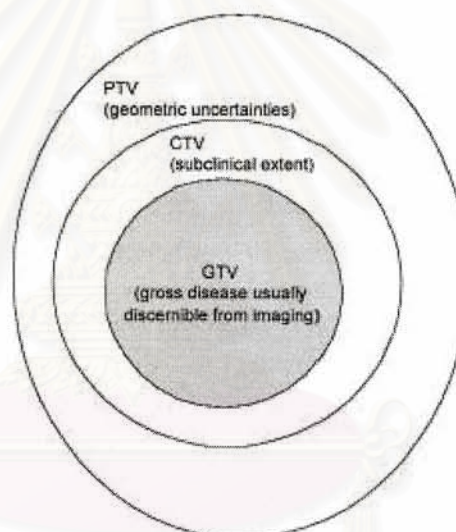
Figure 2.5 The GTV, CTV and PTV concepts from ICRU report 50.
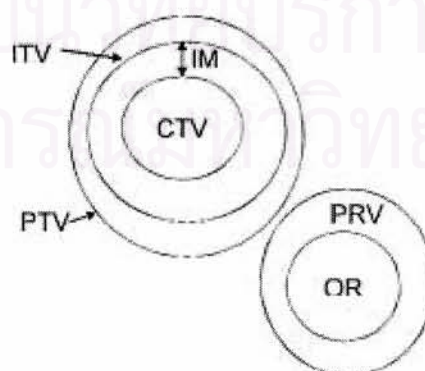
Figure 2.6 The internal margin (IM), internal target volume (ITV), organ at risk (OR), and planning organ at risk volume (PRV) concepts from ICRU report 62.

The internal target volume (ITV) was designed to account for practical issues related to patient treatment. It was considered that intratreatment physiological movement would be difficult to eliminate and, thus, the rules associated with margins for such movement may in fact be different from those for setup variation. The ITV is created by placing an anisotropic internal margin (IM) around the CTV to account for, e.g., breathing movement. Whether all such movements are in fact not manageable is not necessarily critical to the acceptance of the IM and ITV, as this margin can also consider residual error associated with interventions (e.g., gating) to reduce internal movement. Improved understanding and reporting of normal tissue dosimetry is addressed in ICRU report 62 via the constructs of organ at risk and planning organ at risk volume (PRV). The OR represents some internal organ that may be dose limiting and thus needs to be considered in planning and dose reporting. The PRV incorporates and expansion of the OR to account for its movement and setup-induced position change. This construct may be acceptable for absolute assurance that a (serial) organ receives no more than a given point dose. Beyond this, the PRV presents a difficulty that can be generalized to the problem of reporting normal tissue doses, and will be discussed further below. Some investigators have reported that the use of the PRV has enabled IMRT planning with improved reduction of dose to critical structures. It is important to note that most IMRT planning is done with a single representation of the patient, and thus the presence of the PRV may force an unnecessary trade-off.

2.1.4 Expression of uncertainties [8, 9]

Traditionally, an error has been viewed as having two components, namely a random component and a systematic component. According to present definitions, an error is the difference between a measured value and the true value. If errors were known exactly, the true value could be determined; in reality, errors are estimated in the best possible way and corrections are made for them. Therefore, after application of all known corrections, errors do not need any further consideration (their expectation value being zero) and the quantities of interest are uncertainties. An error has both a numerical value and a sign. In contrast, the uncertainty associated with a measurement is a parameter that characterizes the dispersion of the values 'that could reasonably be attributed to the measurand'. This parameter is normally an estimated standard deviation. An uncertainty, therefore, has no known sign and is usually assumed to be symmetrical. It is a measure of our lack of exact knowledge, after all recognized systematic effects have been eliminated by applying appropriate corrections.

2.1.4.1 Geometrical uncertainties [8]

A radiation treatment normally consists of one planning session and multiple irradiation sessions. In the planning phase, the patient geometry is visualized using CT or simulator images. The visualized structures are the basis for construction of the treatment plan and the intention is to deliver this plan in all irradiation sessions. The ICRU considers three sources of geometrical uncertainty that may hamper the exact delivery of a plan: patient set-up variation, organ motion and deformation, and machine related errors. Patient set-up errors are due to variations in the daily positioning of the patient on the treatment couch. Some session-to-session variation is unavoidable, even though several measures are taken to ensure a high reproducibility. Day-to-day tumor motion within the patient can occur due to, for example, variations

in rectum or bladder filling. Cardiac action and respiration can result in intra-fraction tumor movements. With modern radiotherapy equipment, the machine-related geometrical errors, for example in beam sizes and gantry angles, are generally considered small compared to set-up deviations and organ motion.

2.1.4.2 Systematic and random errors [8, 9]

Deviations from the planned irradiation geometry during a treatment session may be systematic or random. Systematic errors occur if the mean irradiation geometry in the fractionated treatment differs from the geometry in the treatment plan. The mean deviations are then called systematic errors. Fraction-to-fraction variations around the mean deviation are called random errors. It should be noted that the source of systematic and random errors can be the same. For example, the patient set-up during acquisition of the planning CT scan may be considered as one sample from the distribution of day-to-day set-ups which will also cause random errors. However, as the geometry in the planning CT scan defines the reference geometry, the set-up at the couch of the CT-scanner will determine the systematic error. The schematic illustration of systematic and random errors is shown in Figure 2.7.
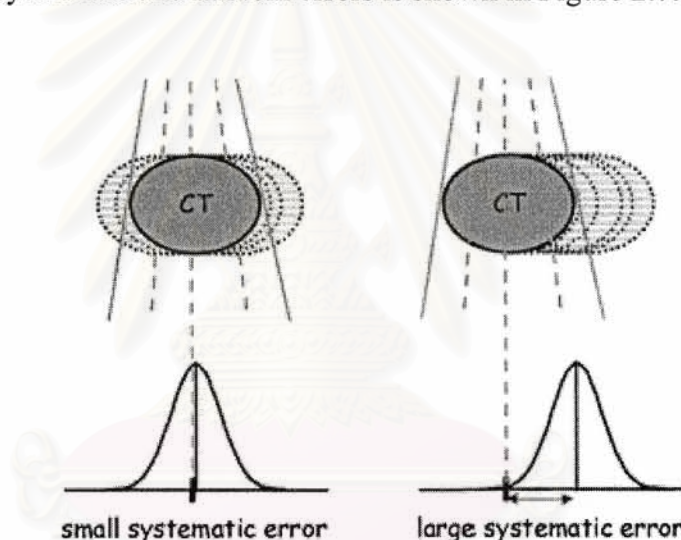
Figure 2.7 Schematic illustration of systematic and random errors. The light gray ellipsoids depict daily tumor positions along one direction. Frequencies of observed tumor positions are indicated by the distribution curves in the two lower panels. The dark gray ellipsoids show tumor positions during acquisition of the CT scan. On the left, that position is close to the average tumor position during treatment, resulting in a small systematic error. On the right, a large systematic error occurs.

For an individual patient, both the systematic and the random errors can only be fully assessed after completion of all treatment fractions. Set-up measurements with an electronic portal imaging device in the first few fractions are sometimes used to estimate the systematic set-up errors, which are then used to drive an off-line correction protocol.

The systematic error represents displacement that was persistent during the whole treatment course. For an individual patient, the systematic error (Σ) was calculated as the average displacement of a particular reference structure and direction between simulation and treatment during the whole treatment course,

$$Systematic\ Error = \sum\nolimits_{ind} = \frac{\sum\limits_{i}^{N} \Delta i}{N} \tag{2.1}$$

where N represents the total number of portal images acquired for a particular field and Δ i is the calculated displacement for the i th treatment fraction.

The random error represents day-to-day variations during treatment course. For each individual patient, the random error (σ) was calculated as the dispersion around the systematic error,

$$Random\ Error = \sigma_{ind} = \sqrt{\frac{\sum\limits_{i}^{N} (\Delta i - \Sigma)^2}{(N-1)}} \tag{2.2}$$

In the traditional categorization of uncertainties it was usual to distinguish between random and systematic contributions. This is undesirable because classifying the components instead of the method of evaluation is prone to ambiguities. For example, a random component of uncertainties in one measurement may become a systematic component of uncertainties in another measurement in which the result of the first measurement is used as an input datum.

2.1.5 Portal imaging [10]

Portal imaging is the use of therapeutic X-ray beam to form an image of the area being irradiated. The historical and current main use of portal images has been the study of setup errors in patient treatment. This has resulted in improved treatment accuracy and in quantification of the margins required to account for the uncertainties in treatment delivery. Margin quantification and reduction is an increasing acceptance that conformal therapy improves patient treatment. Traditionally of portal imaging are megavoltage film and an electronic portal imaging device (EPID). Megavoltage film measurements are rather time consuming and not always very accurate. Over the last years, EPIDs have become available in a large number of institutions.

When the treatment planning is finished the actual treatment execution starts. As mentioned earlier, the treatment is divided into fractions for a curative treatment. Usually the dose is delivered in approximately 30 fractions. This means that the setup of the patient has to be reproduced a large number of times and it must repeatedly be verified that the treatment is in accordance with the plans. It is common practice to control the setup more rigorously in the first couple of fractions to determine if the setup procedure is stable. A Portal Imaging Device (PID) can be used during the treatment to confirm the setup of the patient. These are usually electronic (so called Electronic Portal Imaging Devices or EPIDs) and are placed opposite the gantry on the other side of the couch. The detector rotates together with the gantry. The treatment beam is used similar to an X-ray source and an image of the patient can be recorded. The schematic image of an EPID is shown in Figure 2.8.
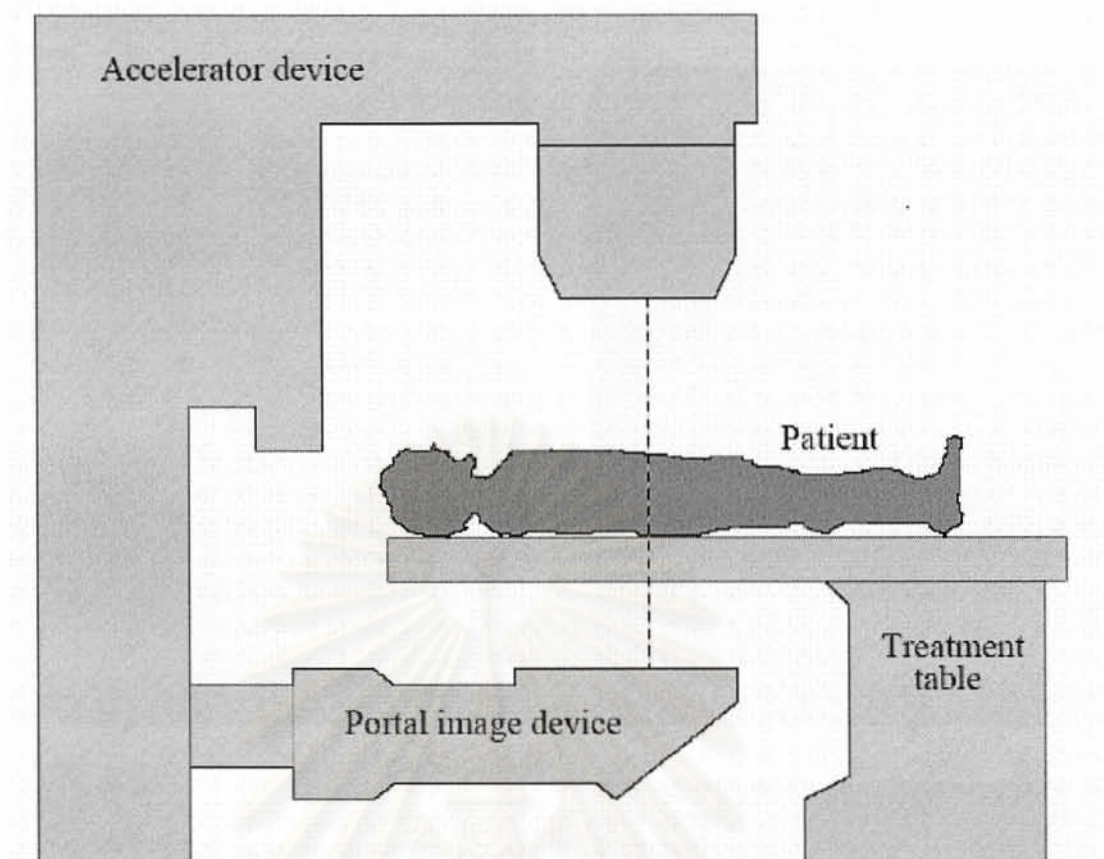
Figure 2.8 Schematic image of an EPID.

2.1.6 Electronic Portal Imaging Device (EPID) [10]

Electronic portal imaging device (EPID), shown in Figure 2.9 was introduced many years ago. They were first used merely as a replacement for port films, but can also be used to exploit the numerous advantages of digital images, in particular the possibility of performing on-line verification. However, clinical acceptance of EPID has been limited by the poor contrast of electronic portal images, as well as extensive history of port film usage. The picture from EPID for patient localization is shown in Figure 2.10.

(a)

(b)

COPYRIGHT ©1999 VARIAN MEDICAL SYSTEMS
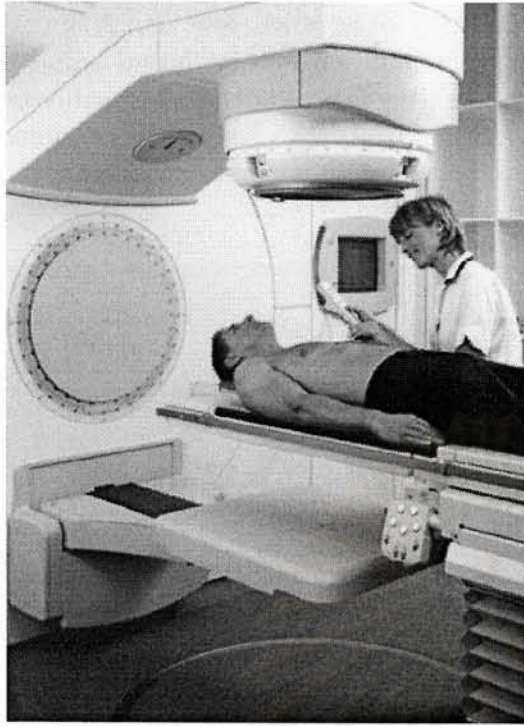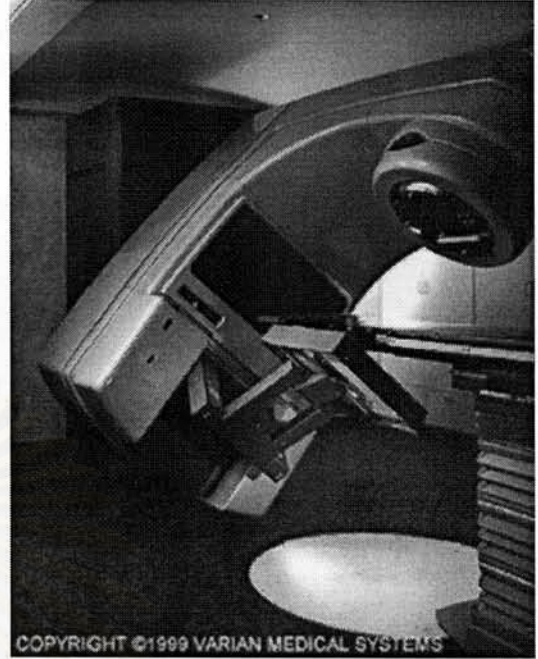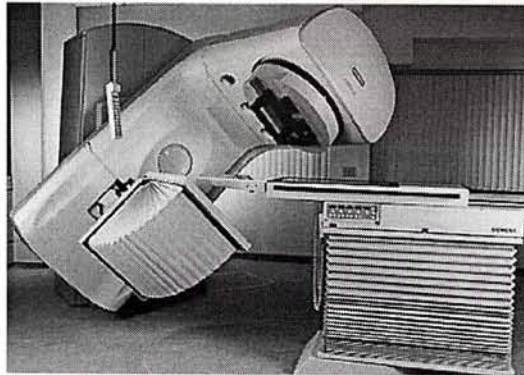
(c)

(d)

Figure 2.9 Electronic Portal Imaging Devices (EPIDs).
(http://bjr.birjournals.org/cgi/content/full/)

A new generation of EPID, based on amorphous-silicon flat panel technology, is being introduced on the market. The new flat panel has fulfilled its promises. It provides high quality portal verification images acquired with as little as 2 cGy (as compared with 7 cGy for film) of dose, while still maintaining comparable quality to our diagnostic reference films.
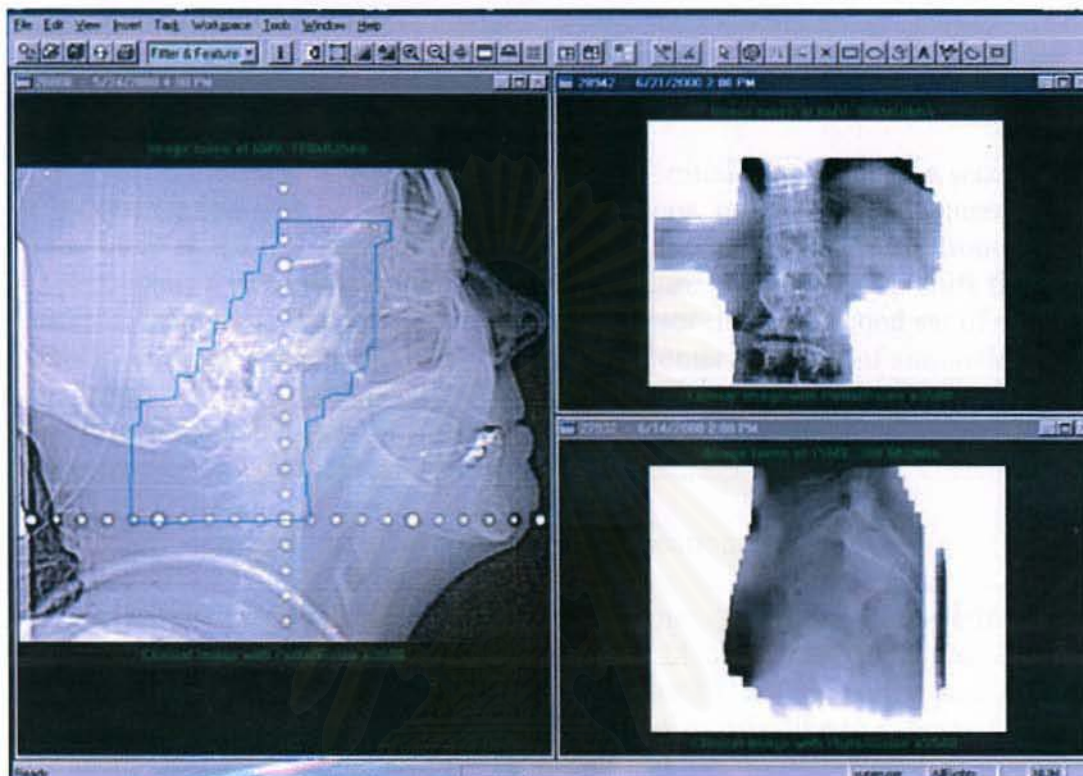
Figure 2.10 The picture from EPID for patient localization.

2.1.7 Treatment Verification [11]

It is essential that all treatment data, including beam configuration and patient information, be directly sent through a local network from a treatment planning system to a record and verify (R&V) system. Initially, it is necessary to verify that there is no treatment information lost or modified during this data transferring process. Due to incorrect default settings in some R&V systems, it is possible that the transferred data could be lost or altered.

2.1.7.1 Patient Setup Verification

With the use of CT simulation during the initial patient setup, a second patient setup verification may be omitted in some situations, provided the treatment isocenter is the same as the CT isocenter. If the treatment isocenter is different from the initial CT isocenter, a patient setup verification procedure is necessary to shift the marked isocenter from the CT isocenter to the treatment isocenter. A second set of orthogonal simulation films is taken using the treatment isocenter. This set of simulation films is compared with the orthogonal DRRs of the treatment isocenter created from the treatment planning system or from the CT simulator, to assure that this newly shifted isocenter agrees with the treatment isocenter.

2.1.7.2 First-Day Treatment Verification

On the first day of treatment, the treatment isocenter is re-verified on the treatment couch. For conventional treatment, the block shapes would also be verified at the same time. For IMRT treatment, whether or not to verify and record the intensity patterns on film is debatable. The physician may like to view and record the treatment regions, similar to the conventional treatment. However, using any commercially available films, it is difficult to obtain a good quality image with an intensity pattern superimposed on the patient anatomy information. For example, if IMRT is delivered with static MLC, an intensity pattern is composed of a series of segments, each assigned with a different monitor unit (MU). Directly delivering the treatment intensity pattern to any type of commercially available films cannot obtain an image with good contrast for both the intensity pattern and patient anatomy, even with an added open field using up to 5 MUs at the end of each beam direction. Alternatively, using the regular portal film, one can record the outer boundary of the intensity pattern as a substitute for the block shape in conventional treatment, although the intensity variation across the field is not recorded. Unfortunately, most commercial treatment planning systems do not provide tools for obtaining a special field (let us say portal film field) with the outside boundary of each intensity pattern. Some institutions have developed in-house software to create such a special portal film field for each beam direction.

2.1.7.3 Effect of Patient Position and Motions

With the introduction of IMRT and its conformality around the tumor volume, more rigid immobilization devices have been designed and implemented for head and neck IMRT treatment. Similarly, various groups have also closely studied patient setup variation and the subsequent dosimetric effects. A study simulating possible dosimetric effects of patient displacement and collimator and gantry angle

misalignment on IMRT showed that a 3 mm movement in anterior-posterior (AP) positioning could contribute up to a 38% decrease in the minimum target dose [12]. Another study determined that with 5 mm translational shifts in all six directions [superior-inferior (SI), AP, and right lateral (RL)], the incorporation of planning organ at risk volume (PRV) could indeed decrease the average volume of contralateral parotid receiving greater than 30 Gy from 22% to 4% [13].

2.2 Related literatures

Several authors have examined the degree of interfraction variability for patients being treated for head and neck cancer, however, the degree of deviation varies from institution to institution. Hurkmans et al. [14] reviewed a large number of studies regarding the current clinical practice of set-up verification using portal imaging. The reported set-up accuracy varied widely, depending on the treatment site, method of immobilization and institution. The standard deviation (1 SD, mm) of systematic and random errors for their currently applied treatment techniques, separately measured along the three principle axes, ranges from 1.6-4.6 and 1.1-2.5 (head and neck), 1.0-3.8 and 1.2-3.5 (prostate), 1.1-4.7 and 1.1-4.9 (pelvis), 1.8-5.1 and 2.2-5.4 (lung), and 1.0-4.7 and 1.7-14.4 (breast), respectively. Recommendations for procedures to quantify, report and reduce patient set-up errors were also given. Using their recommendations, the systematic and random set-up errors that can be achieved in routine clinical practice could be less than 2.0 mm (1 SD) for head and neck, 2.5 mm (1 SD) for prostate, 3.0 mm (1 SD) for general pelvic and 3.5 mm (1 SD) for lung cancer treatment techniques.

Hess et al. [15] studied the accuracy of the field alignment in 95 head and neck patients immobilized with a facial mask. Measurements were made from identifiable anatomic landmarks to the field edges on simulation and portal films to determine setup variation. All measured deviations were normally distributed, with mean values of 0 to 3 mm and standard deviations of 3 to 5 mm. of the absolute deviations, 50% and 90% were within 3 mm and 9 mm, respectively, and about 20% of the absolute deviations exceeded 5 mm.

Huizenga et al. [16] determined the accuracy of radiation field alignment for a group of 22 patients with tumors in the head and neck. The accuracy was assessed by an analysis of 138 megavolt portal films in comparison to 55 simulation films. The distance (at the patient midplane) between corresponding points at the field edges on verification film and simulation film appeared to be 5 mm on the average and the standard deviation of 5 mm. The analysis was extended by translational and rotational matching of the fields in order to separate each error in a translation error of the field with respect to the patient and an error in field size or shape. Translation errors appear to be somewhat larger than field size or shape errors. From an analysis of a series of megavolt films taken every third radiotherapy session, it was concluded that treatment-to-treatment variations were as large as the errors due to the transition from simulation to treatment situation. Further analysis showed that variation of the patient's position within the cast was clearly one of the error sources.

Gilbeau et al. [17] compared the setup accuracy of three different thermoplastic masks used for immobilization of patients with brain or head and neck tumors. Thirty patients with brain or head and neck tumors were consecutively assigned to one of three different thermoplastic masks (Posifix): head mask with three fixation points (FP) (3 FP, ten patients), head and shoulder mask with four fixation points (4 FP, ten patients), head and shoulder mask with five fixation points (5 FP,

four fixations plus an additional one on the top of head, ten patients). Once a week, during the session with a 6 MV linac (Elekta), orthogonal (antero-posterior and lateral) portal images were acquired for three fictitious isocenters placed during the simulation at the level of the head, the neck and the shoulders. Portal images and digitized simulator films were compared using the PIPS pro software, and displacements in antero-posterior (A-P), cranio-caudal (C-C) and medio-lateral (M-L) directions were calculated. From these displacements, 2D or 3D errors were also calculated. A total of 915 portal images were obtained, 98% of which could be analyzed. For the whole population, total displacements reached a standard deviation (SD) of 2.2 mm at the level of the head and the neck. Systematic and random displacements were in the same order of magnitude and reached a SD of 1.8 mm. Patient setup was slightly worse at the shoulder level with a total displacement of 2.8 mm (1 SD) for both the C-C and the M-L directions. There again, the systematic and the random components were in the same order of magnitude below 2.4 mm (+/-SD). For isocenters in the head and in the neck, there was no substantial difference in the setup deviation between the three masks. The setup reproducibility was found to be significantly worse (P=0.01) at the level of the shoulders with the 3 FP mask. For the 2D random error, 1 SD of 2.3 mm was observed compared to 0.8 and 1.2 mm for the 4 and 5 FP masks, respectively. Lastly, 90% of the 3D total deviations were below 4.5 mm for the head and the neck. In the shoulder region, 90% of the 2D total deviations were below 5.5 mm. Thermoplastic masks provided an accurate patient immobilization. At the shoulder level, setup variations were reduced when 4 or 5 FP masks were used. These data could be used for the assessment of margins for the PTV.

Assessments of clinic and site specific margins are essential for the effective use of three-dimensional and intensity modulated radiation therapy. Prisciandaro et al. [9] studied a methodology to determine margins by EPID measurements of patient setup variation and motion as applied to immobilization devices. Although the full study involved the use of an EPID-based method to assess the impact of (1) simulation technique, (2) immobilization, and (3) surgical intervention on inter- and intrafraction variations of individual and population-based CTV-to-PTV margins, the focus of the paper was on the technique. As an illustration, the methodology was utilized to examine the influence of two immobilization devices, the UON™ thermoplastic mask and the Type-S™ head/neck shoulder immobilization system on margins. Daily through port images were acquired for selected fields for each patient with an EPID. To analyze these images, simulation films or digitally reconstructed radiographs (DRR's) were imported into the EPID software. Up to five anatomical landmarks were identified and outlined by the clinician and up to three of these structures were matched for each reference image. Once the individual based errors were quantified, the patient results were grouped into populations by matched anatomical structures and immobilization device. The variation within the subgroup was quantified by calculating the systematic and random errors. Individual patient margins were approximated as 1.65 times the individual-based random error and ranged from 1.1 to 6.3 mm (A–P) and 1.1 to 12.3 mm (S–I) for fields matched on skull and cervical structures, and 1.7 to 10.2 mm (L–R) and 2.0 to 13.8 mm (S–I) for supraclavicular fields. Population-based margins ranging from 5.1 to 6.6 mm (A–P) and 3.7 to 5.7 mm (S–I) were calculated for the corresponding skull/cervical field and 9.3 to 10.0 mm (L–R) and 6.3 to 6.6 mm (S–I) for the supraclavicular fields, respectively. The reported CTV-to-PTV margins are comparable to a value 7–15 mm based on traditional Mayo margins, but in some cases exceed the default values

established in RTOG Head-and-Neck studies. The data suggested that the population-based margins provided sufficient coverage for the majority of their patients. However, the population-derived margins were excessive for some patients and insufficient for others, suggesting that a re-evaluation of current treatment margins for individual patients was warranted. Finally, this methodology provided direct evidence of treatment variation and thus can demonstrate with confidence, the superiority of one technique over another.

CHAPTER 3

RESEARCH METHODOLOGY

3.1 Research Design

This study is descriptive cross sectional study research.

3.2 Research Questions

3.2.1 Primary Research Question
How much is the setup variation in IMRT of head and neck cancer in Division of Radiation Oncology at King Chulalongkorn Memorial Hospital?

3.2.2 Secondary Research Question
How much is the adequate CTV-to-PTV margin in IMRT of head and neck cancer in Division of Radiation Oncology at King Chulalongkorn Memorial Hospital?

3.3 Research Design Model

```
┌──────────────┐                              ┌──────────────┐
│ Radiographic │                              │     EPID     │
│  simulation  │                              │              │
└──────┬───────┘                              └──────┬───────┘
       │                                             │
       ▼                                             ▼
  ╭──────────╮      ┌──────────────────┐       ╭──────────╮
  │Radiographic│───▶│VARiSVision software│◀──── │ Portal   │
  │ simulation │     └─────────┬────────┘       │  image   │
  │   image    │               │                ╰──────────╯
  ╰──────────╯                 ▼
                     ┌──────────────────┐
                     │Anatomical matching│
                     └─────────┬────────┘
                               │
  ┌──────────────┐    ┌──────────────┐    ┌──────────────┐
  │ Random error │◀───│  Isocentric  │───▶│Systematic error│
  └──────┬───────┘    │  deviation   │    └──────┬───────┘
         │            └──────────────┘           │
         │     ┌──────────────────────────┐      │
         └────▶│ Determine the setup error │◀─────┘
               │ (Individual and population)│
               └─────────────┬────────────┘
                             ▼
               ┌──────────────────────────┐
               │    Population-based       │
               │   margin calculation      │
               └─────────────┬────────────┘
                             ▼
           ┌──────────────────────────────────┐
           │Comparison to a value 5-10 mm based│
           │         on traditional use in     │
           │ King Chulalongkorn Memorial Hospital│
           └─────────────┬────────────────────┘
                         ▼
               ┌──────────────────────────┐
               │    Define adequate        │
               │   CTV-to-PTV margins      │
               └──────────────────────────┘
```

3.4 Conceptual Framework

```
┌─────────────────────┐                    ┌──────────────────────────────┐
│ Deviation between   │                    │    Deviation between         │
│ different fractions │                    │ the planned patient position │
│                     │                    │ and the average patient      │
│                     │                    │ position                     │
└─────────────────────┘                    └──────────────────────────────┘
          │                                              │
          ▼                                              ▼
┌─────────────────────┐                    ┌──────────────────────────────┐
│ Random error        │                    │    Systematic error          │
│ (Interfraction      │                    │                              │
│ variation)          │                    │                              │
└─────────────────────┘                    └──────────────────────────────┘
          │                                              │
          └──────────────►┌─────────────────┐◄──────────┘
                          │ Setup variation │
                          └─────────────────┘
                                   │
                                   ▼
                          ┌─────────────────────┐
                          │ Margin calculation  │
                          └─────────────────────┘
                                   │
                                   ▼
                          ┌─────────────────────┐
                          │ Population-based     │
                          │ CTV-to-PTV margins  │
                          └─────────────────────┘
                                   │
                                   ▼
                          ┌─────────────────────┐
                          │ Define adequate      │
                          │ CTV-to-PTV margins  │
                          └─────────────────────┘
```
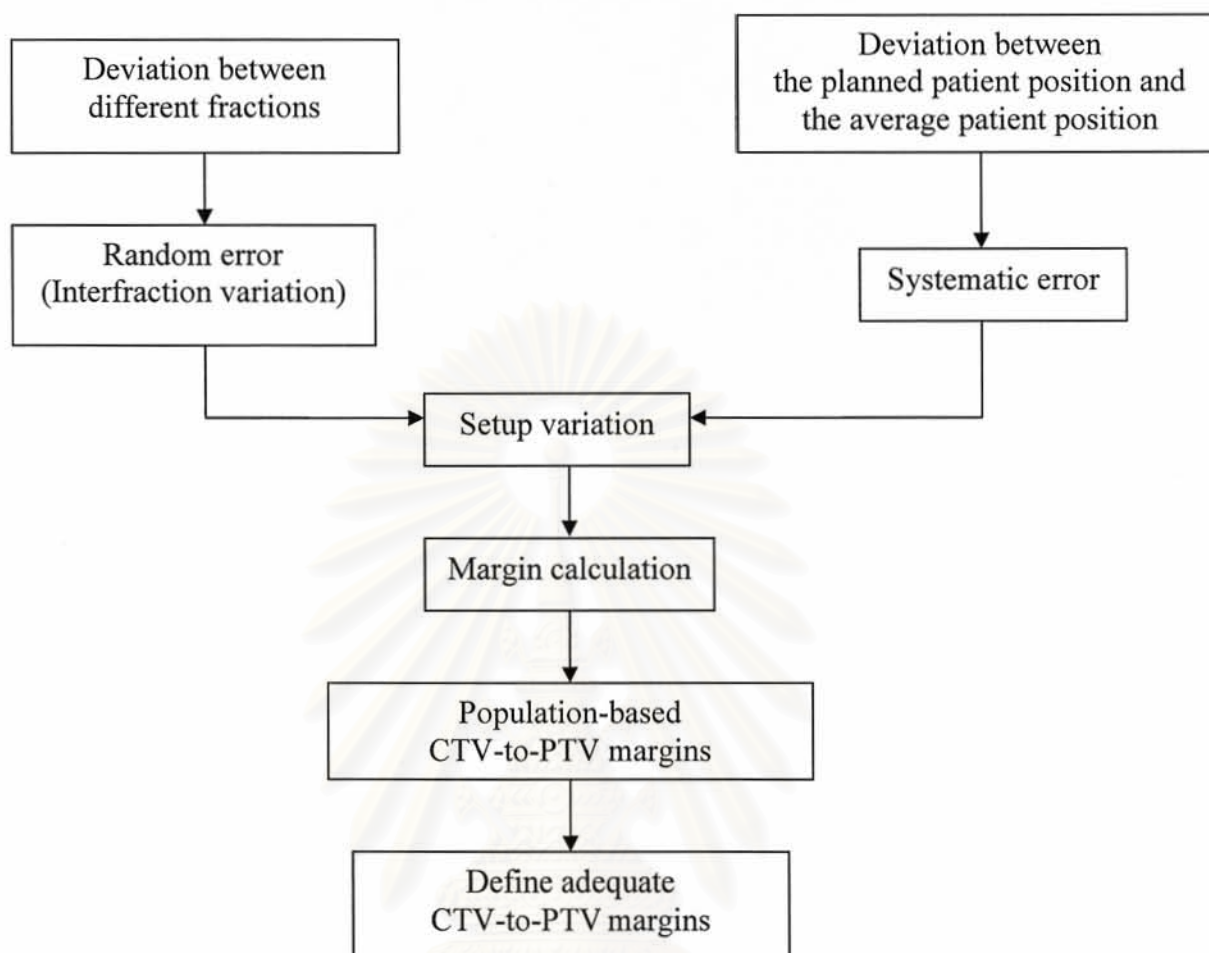
3.5 The Sample

The patients who underwent IMRT of head-and-neck cancer at King Chulalongkorn Memorial Hospital from March 1st to November 30th, 2006 were recruited.

3.6 Materials

3.6.1 Linear accelerator

The Varian Clinac 23EX linear accelerator (Varian Oncology Systems, Palo Alto, CA, USA), is shown in Figure 3.1, with dual photon beam of 6 MV and 15 MV, and six electron beam energies of 4, 6, 9, 12, 16 and 20 MeV. The photon beam of 6 MV was used in this experiment. Photon field sizes are range from 0.5 x 0.5 cm^2 to 40 x 40 cm^2 at isocenter. The distance from the target to isocenter is 100 cm. There are six stationary therapy dose rates range from 100-600 monitor units per minute, 300 MU/min was used for the treatment in this institute. The multileaf collimator (MLC) is mounted below the conventional collimator in the same direction of x-jaws. There are 120 leaves that can move as the dynamic movement.

Figure 3.1 Varian Clinac 23 EX.

3.6.2 Electronic Portal Imaging Device (EPID)

The amorphous silicon aS500 EPID (Varian Oncology Systems, Palo Alto, CA, USA) is shown in Figure 3.2, it consists of a 1 mm copper metal plate, a 134 mg/cm^2 gadolinium oxysulphide phosphor screen (Kodak, Lanex Fast B) that includes a 0.18 mm polyester reflector, and a 40 x 30 cm^2 (512 x 384 pixel) a-Si array. Each pixel consists of a light sensitive photodiode and a thin film transistor with a pixel pitch of 0.78 x 0.78 mm^2. The copper plate lies beneath a 10 mm thick foam layer with 1 mm of epoxy for binding. The scintillator and amorphous silicon array (~1mm thick) are bound to the underside of the copper plate and are enclosed between thin layers of black paper to prevent light scatter from the copper plate or components beneath the array, reaching the array. Beneath this lies a further 8 mm foam and 1 mm epoxy. A 1.6-mm-thick plastic collision cover (epoxy with glass and foam) encloses the detector with an air gap of approximately 1.5 cm between the cover and the detector surface. The EPID was integrated with a linear accelerator with a dynamic multileaf collimator (DMLC).

Figure 3.2 The amorphous silicon EPID.

3.6.3 Simulator

The Acuity simulator (Varian Oncology Systems, Palo Alto, CA, USA) is used to simulate the set up of the patient treatment fields as treatment units do. The Acuity simulator is shown in Figure 3.3. Acuity's amorphous silicon panel produces high-resolution, distortion-free images. The 40 cm x 30 cm panel accommodates most field sizes, and images can be acquired without having to move the imager. It integrated with the information network (Varian VARiSVision version 7.3.10).
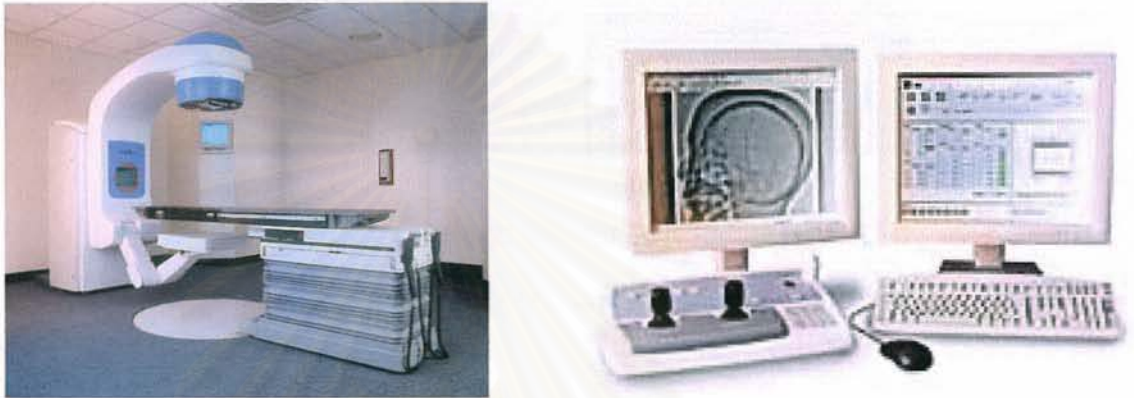
Figure 3.3 The Acuity simulator.

3.6.4 CT simulator

The LightSpeed RT CT simulator scanner (GE Medical systems, Milwaukee, WI, USA) is used to localization and field design with direct transfer of information from the CT simulator to other information systems within the radiation oncology department. CT images, coordinate system definitions, contour information and field parameters can be transferred to and from the treatment planning system. The picture is shown in Figure 3.4. AdventageSIM provides complete volume definition and geometric beam placement capability for radiotherapy. It is then able to compute a real time DRR for any type of patient setup and can fully replace a classic X-ray simulator for treatment setup reference image generation. It is the ability to simultaneously collect 4 rows of scan data. This 4-row data collection is accomplished via a 16-row detector and a 4-row DAS. The distance from tube to imaging isocenter is 606 mm. The distance from tube focus to detector is 1062 mm. Remote tilt gantry from operator console is ±30°. The maximum SFOV is 65 cm. Bore diameter is 800 mm. An x-ray tube has A Tungsten-Rhenium focal track on a molybdenum alloy substrate back by graphite target with maximum heat capacity of 7.5 MHU. Four kVp settings are available (80, 100, 120 and 140 kVp). Exposure techniques range from 10 to 400 mA in 5-mA increments with five scan time setting (1, 2, 3, 4s) and seven reconstruction algorithms (soft, standard, lung, detail, bone, edge and bone plus).

Figure 3.4 The CT simulator scanner (GE LightSpeed RT).

3.6.4 PortalVision ATP Phantom (Varian Oncology Systems, Palo Alto, CA, USA) Part.Ident.No.B01393-01A

The ATP phantom is designed to check the quality of image of EPID. The PortalVision ATP Phantom is shown in Figure 3.5.

Figure 3.5 PortalVision ATP Phantom (Portal Vision [TM], Varian medical system).

3.6.5 Perspex (PMMA) Phantoms

The perspex (PMMA, Wellhofer, Bavaria, Germany) phantom (density = 1.03 g/cm^3, atomic number = 5.97) is made in square slab of 30 x 30 cm^2 with the thickness of 5.0 cm. The perspex (PMMA) phantom was designed to measure the accuracy of software by placing the catheter wire on field edge and center of 10×10 cm^2 field size on top of perspex and at the center thickness. The picture is shown in Figure 3.6.

Figure 3.6 The Perspex (PMMA) Phantoms.

3.6.6 The TYPE-S^{TM} head/neck shoulder immobilization system

The TYPE-S^{TM} (MED-TEC Incorporated, IA, USA) is a head/neck shoulder immobilization system, shown in Figure 3.7. This device conforms to the patient's head, neck and upper shoulders. The Type-S system was developed to offer a higher degree of stability for the neck and shoulders. The baseplate is a carbon fiber grid that extends off the end of CT simulator, simulator, or treatment couch. Attenuation through the carbon fiber base and treatment grid is minimal and portal image friendly. The Type-S baseplate can be locked to simulator, CT simulator, and treatment couchtops for precise and reproducible setups from simulation through delivery.

Figure 3.7 The TYPE-S^{TM} (MED-TEC Incorporated, USA).
(http://www.medtec.com/products/immobilization/hn/type-s/default.htm)

3.6.7 Eclipse treatment planning system.

Eclipse (Varian Oncology Systems, Palo Alto, CA, USA) is a treatment planning system for all modalities such as 3D conformal, Intensity Modulated Radiation Therapy (IMRT), electron and brachytherapy. Advanced processes such as Image Guided Radiation Therapy (IGRT) and Dynamic Adaptive Radiation Therapy (DART) are supported. The properties of Eclipse treatment planning system is shown in Figure 3.8

External Beam Planning 6.5

Application Build: 7.3.10   [SP 3]
Server Build: 7.1.67.3   [SP 13]

VAR*I*AN
medical systems

Copyright © 1996 - 2004 Varian Medical Systems, Inc.

ICD-O codes and terms © World Health Organization, 2000
ICD-10 codes and terms © World Health Organization,

CE 0086

Legal Manufacturer

Varian Medical Systems Inc.,
Worldwide Headquarters
3100 Hansen Way,
Palo Alto, CA 94304
USA

European Representative

Varian Medical Systems UK Ltd,
Gatwick Road
Crawley
West Sussex, RH10 9RG
United Kingdom

System Info ...   OK

Figure 3.8 Eclipse treatment planning system.

5.6.8 VARiS Vision (Version 7.3.10) software

VARiS Vision software simplifies the many steps involved in delivering a
multi-week course of radiation therapy, including treatment planning, simulation,
scheduling, patient positioning, treatment delivery, verification, and quality assurance.
The VARiS Vision system incorporates DICOM to link with the simulator, CT
simulator, treatment planning and linear accelerator. The information of image and
data could be transfer between the set of Varian therapy machines. The clinicians can
control the full treatment delivery process and have images immediately available for
review. While imaging will certainly facilitate treatment planning, they also will
impact treatment verification. The VARiS Vision software is shown in Figure 3.9.
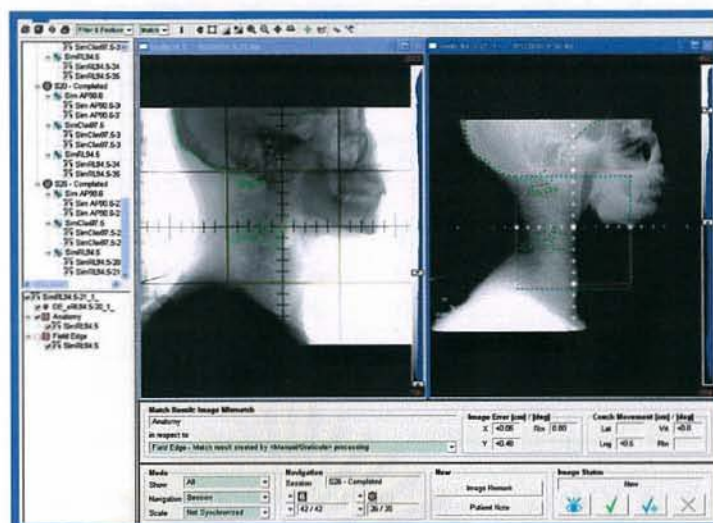
Figure 3.9 VARiS Vision (version 7.3.10) software.

3.7 Methods

This study was performed on 9 head and neck cancer patients, treated with dynamic IMRT, 6 MV x-ray beam from VarianClinac 23EX of 120 leaves MLC at King Chulalongkorn Memorial Hospital from March 1st to November 30th, 2006. Treatment fields encompass primary tumor as well as lymph nodes at risk. All the patients were immobilized with TYPE-S^{TM} thermoplastic mask covering head, neck and shoulders, which was fixed to the treatment couch. Prior to treatment all patients had three images of setup field which were two orthogonal, anterior-posterior (AP) and lateral image at the upper neck level, and the other AP field at the shoulder level. The simulator images were acquired on the Acuity digital simulator and transferred into VARiSVision as the reference images. Weekly portal images of three setup fields which were the same fields as taken with the simulator were acquired for each patient with amorphous silicon EPID. Images were taken and assessed during the first week of treatment and weekly thereafter. The images were then transfered to VARiSVision to compare with the reference images.

The procedure was performed in the following sequence.

3.7.1 Quality control

3.7.1.1 Quality check of EPID (Contrast detail resolution)

Contrast detail resolution defines the imager's ability to display objects with low contrast for a given energy and dose. It is determined by taking images of the PortalVision ATP phantom at each energy. The different hole depths correspond to different object contrasts visible at a given low contrast for a certain beam energy and dose. Object contrast here is a physical contrast.

The lists of the object contrast in percentage for the various hole depths of the PortalVision ATP phantom as a function of the photon energy is shown in Table 3.1. The holes of the PortalVision ATP phantom corresponded to the object contrast detail resolution.

Table 3.1 Percentage of object contrast which determined by using PortalVision ATP phantom as a function of hole depth (mm) and photon energy (MV) was defined by the difference over the sum of the transmissions.

	4 MV	6 MV	8 MV	10 MV	15 MV	18 MV	25 MV
3 mm	2.25%	1.75%	1.50%	1.33%	1.05%	1.05%	0.97%
2 mm	1.50%	1.17%	1.03%	0.89%	0.76%	0.70%	0.65%
1 mm	0.75%	0.59%	0.52%	0.44%	0.38%	0.35%	0.33%
0.5 mm	0.38%	0.30%	0.27%	0.23%	0.19%	0.18%	0.17%
	0.19%	0.15%	0.13%	0.11%	0.10%	0.09%	0.08%

The object contrast resolution shall be ≤ 0.2 % at 6 MV, for the largest holes at a minimum dose per frame of 0.5 MU. In other words, as 6 MV an object contrast ≥ 0.2 % shall be visible. This corresponds to a measured displayed contrast as shown by the image in Figure 3.10
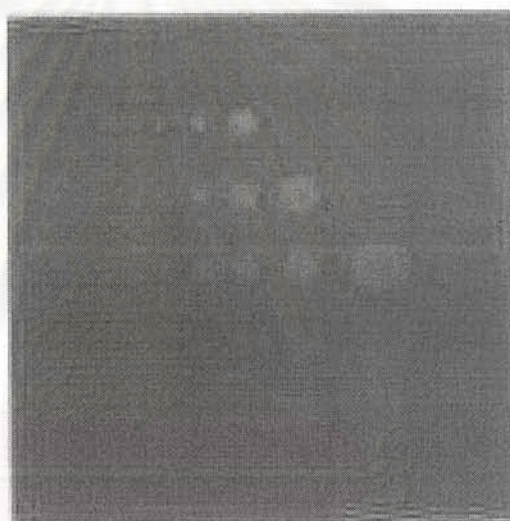
Figure 3.10 Typical PV Phantom image (6 MV).

The PortalVision ATP phantom and the holes that shall be visible at least are shown in Table 3.2 and Figure 3.11. This depends on the various photon energies and is specified for a minimum dose per frame of 0.5 MU. Only the first holes of each horizontal line are considered because the other holes on the same line have the same depth and therefore correspond to the same object contrast.

Table 3.2 Low contrast spatial resolution specification for aS500 with the PortalVision phantom at isocenter.

Photon Energy (BJR 11)	Holes at least visible in PV Phantom
4 MV	A, B, C, D, E
6 MV	A, B, C, D, E
8 MV	A, B, C, D, E
10 MV	A, B, C, D
15 MV	A, B, C, D
18 MV	A, B, C, D
25 MV	A, B, C, D
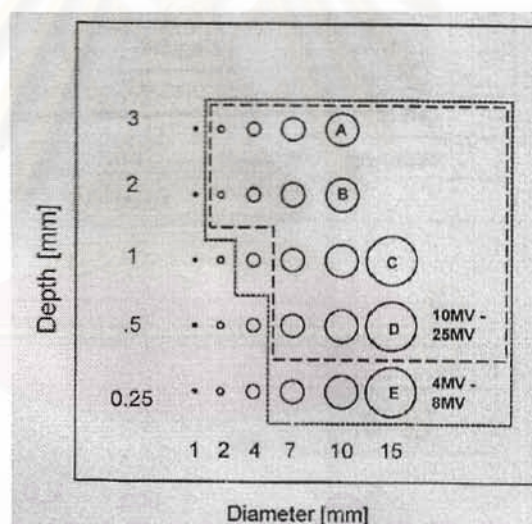
Figure 3.11 Low contrast spatial resolution specification for aS500 with the PortalVision phantom at isocenter, for an image minimum dose per frame of 0.8 MU and 10 frames (high quality) with the detector at 140 cm.

The low contrast spatial resolution was checked by place PortalVision phantom at the isocenter height (middle of the phantom thickness at isocenter) with the detector at 140 cm and oriented in order to have the displayed images as shown in Figure 3.10. The deepest (3 mm) and smallest (1 mm) holes are displayed at the upper left corner of the image.

3.7.1.2 Accuracy check of VARiSVision software

EPID is used in quantitative evaluation of patient setup, accuracy check involves measurement of known setup errors. These measurements were designed to separate the results into those based on field placement and the location of the phantom in the field. The effects of image processing (e.g. image enhancement and edge detection) on the accuracy of setup analysis were established. Image processing may affect the results of quantitative reporting. The process include understanding and characterizing the limits of reference image generators (simulators, DRRs, etc.), since field placement errors are determined by comparing portal images to reference images.

A test was performed to determine the ability of the system to reproduce a null transform on identical images. It is best to use the EPID's own software to compare an image to itself. Typical accuracy for such tests has ranged from 0.5 mm to 2 mm.

In this study, the perspex (PMMA) phantom was attached with the marker designed to measure the accuracy of VARiSVision software in our division as shown in Figure 3.5. The perspex (PMMA) phantom was placed at the isocenter of CT simulator and VarianClinac23EX as shown in Figure 3.12. The treatment planning was performed. Displacements of isocenter in all directions were measured on anterior and lateral portal images. The image was analyzed and recorded mismatch data.

(a) CT Simulator

(b)Varian Clinac23EX
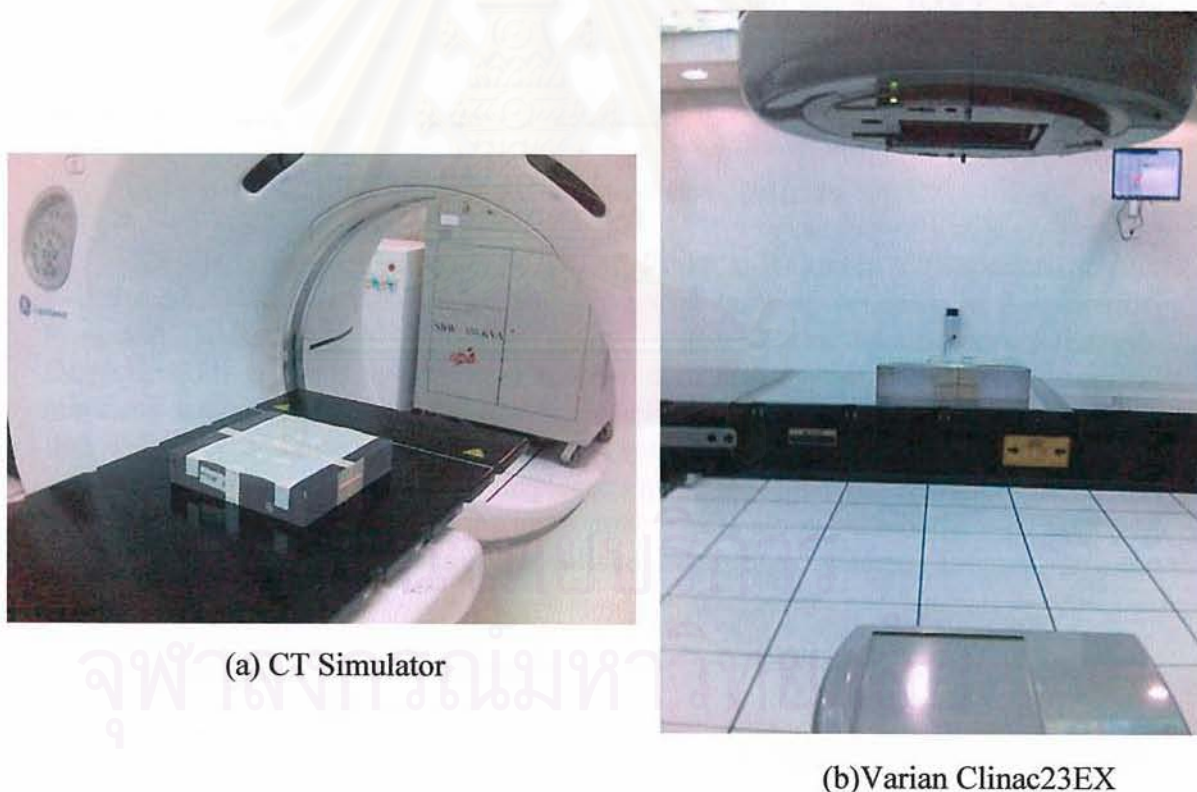
Figure 3.12 The perspex (PMMA) phantom is placed at the isocenter of
(a) CT Simulator and (b) Varian Clinac23EX.

3.7.2 Portal image analysis by anatomical matching

All portal images were matched with the reference images using the VARiS Vision software that provided a tool for automatic image registration (Anatomy Matching or Automatic Matching). The software then automatically calculates the magnification factors allowing direct comparison between the reference and portal images. It also allowed improvement of the image quality with different filters and contrast enhancement tools. Comparison between a simulator image set as reference image and a portal image was performed using "Anatomy Matching". The idea of "Anatomy Matching" is to find a small patch of image around each point in the reference that matches an identical patch in the portal image. In this study, we created a match anatomy layer that was required for the matching process.

Anatomical contours of bony landmarks which were skull bones, the first cervical vertebral body (C1) and the fourth cervical vertebral body (C4) for lateral field and mandible, clavicle and spinous process for anterior field were drawn manually on each reference image. Then the system aligned the portal images and the reference image anatomically according to the defined match points on the match anatomy layer. An anatomy match object was produced and superimposed on the portal image. The patient misalignment was indicated in the Image Mismatch panel as shown in Figure 3.12-3.14. The software in VARiSVision can calculate the coordinates of six bony landmarks relative to the isocenter. Verification of the isocenter was carried out for the first treatment day of the IMRT and weekly thereafter. Since the magnitudes of the movement of head and neck tumors may vary according to the location of the tumors, the position of each of six visible bony landmarks relative to the isocenter was evaluated.

3.7.2.1. Setup error for head-and-neck patients

Displacements of isocenter in X (Left-Right, L-R) and in Y (Superior-Inferior, S-I) directions were measured on anterior portal images, whereas, in Z (Anterior-Posterior, A-P) and Y direction were measured on lateral portal images. Displacements in all direction were measured in millimeters. After the anatomical matching was performed on the treatment fields for an individual patient, mismatch data were recorded into a Microsoft® Excel spreadsheet.

The reported X, Y and Z displacement of isocenter between simulation and treatment was decomposed into the appropriate shifts along each body axis. Superior, right and posterior movements were defined as negative whereas inferior, left and anterior as positive.
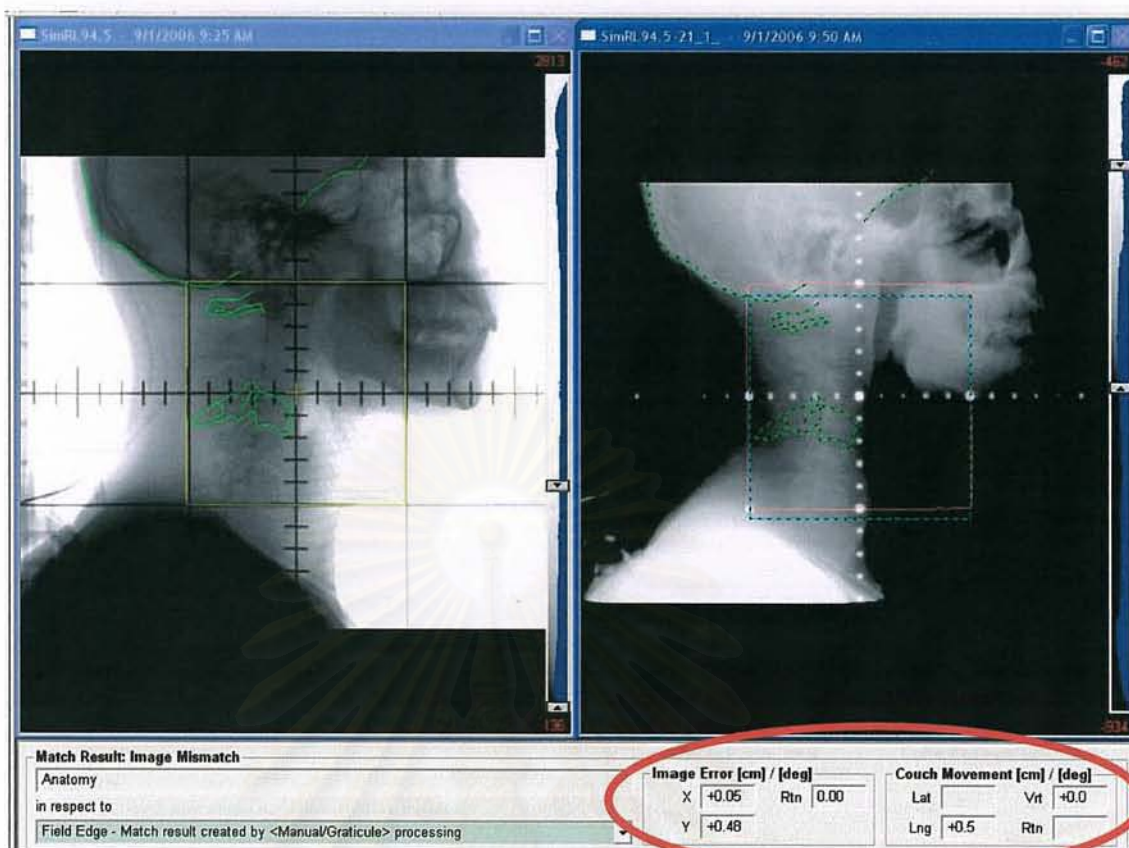
Figure 3.12 (Left) Simulator image of a right lateral setup field with contours outlined skull bones, C1 and C4. (Right) Corresponding treatment portal image matched to skull bones. An additional match was performed on this image to C1 and C4.
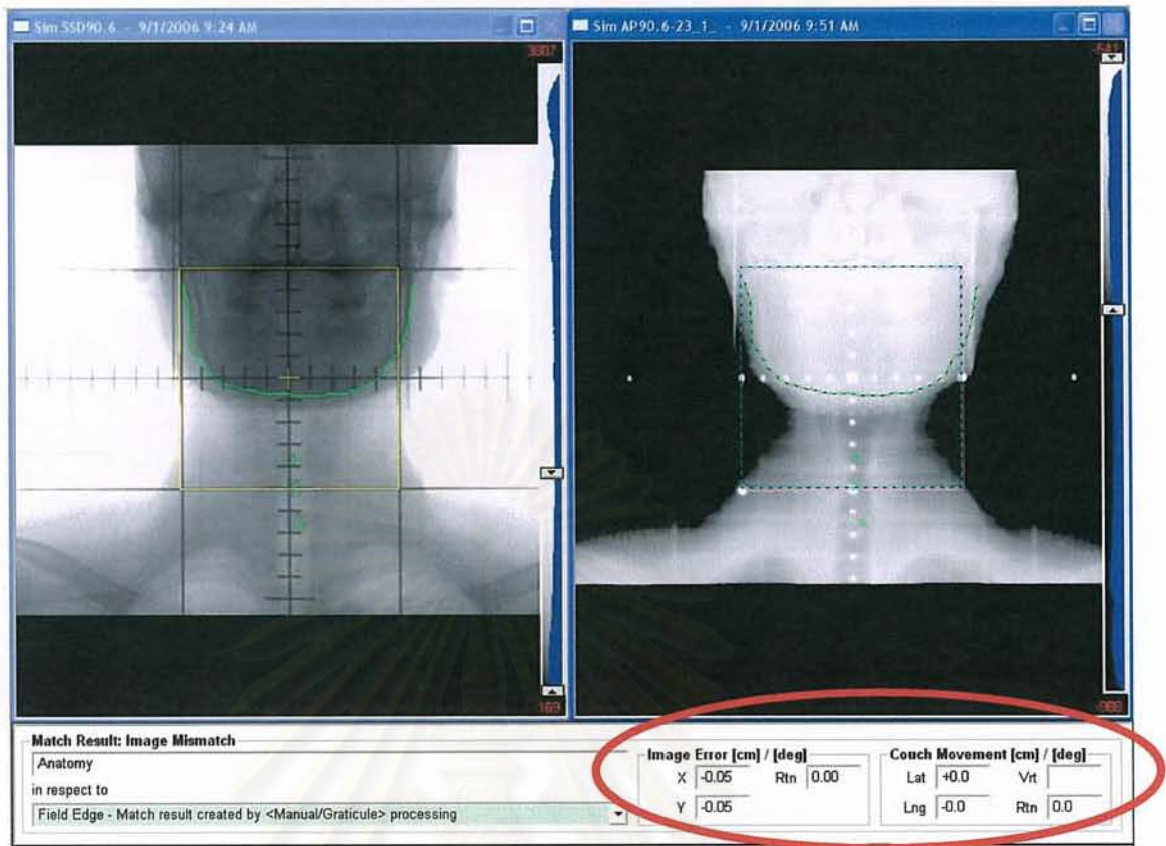
Figure 3.13 (Left) Simulator image of an anterior setup field with contour outlined mandible and spinous process. (Right) Corresponding treatment portal image matched to mandible. An additional match was performed on this image to spinous process.
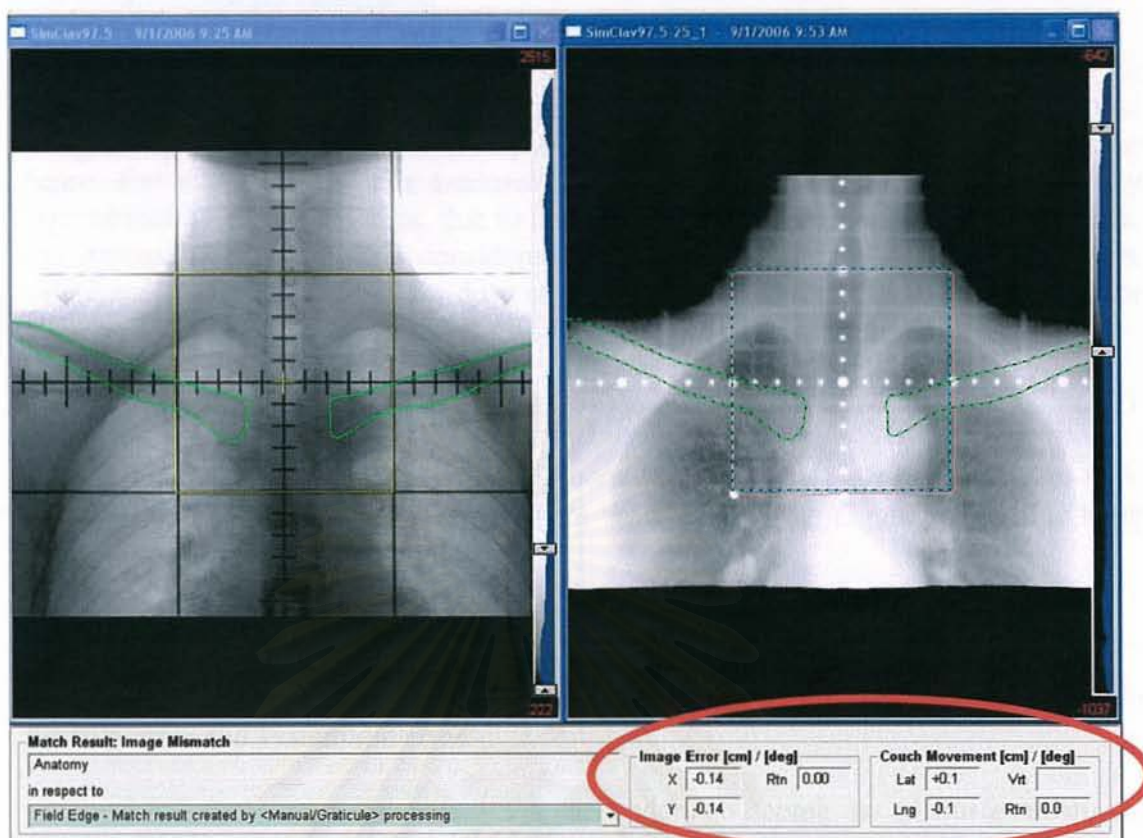
Figure 3.14 (Left) Simulator image of an anterior setup field at shoulder level with contour outlined clavicle. (Right) Corresponding treatment portal image matched to clavicle.

3.7.2.2. Systematic error and random error for individual patient and population

In the overview of errors in radiotherapy, errors were classified as systematic and random. Suppose that we have measured an error on a weekly basis for a number of patients and fractions.

For each individual patient, measurement of the displacement between simulator image and one single treatment session represents the total variation in patient positioning for the treatment session considered. Displacements of the coordinates of each landmark in the portal image from those in the simulation images were determined as setup error for each bony landmark. The displacements were used to calculate the systematic and the random error following the equation of Prisciandaro et al [9] by Eq. (2.1) and Eq. (2.2) in page 14 chapter 2.

For the whole population, the population systematic errors (Σ_{pop}) for a particular isocenter and direction were expressed by the standard deviation (SD) from the values of the average displacement of all individual patients (Σ_{ind}). While the population random error was expressed by the SD from all individual random error (σ_{ind}) [8].

3.7.3 Margin calculation

According to ICRU report 62 [1], the CTV-to- PTV margin should account for internal motion and variations in the size, shape, and position of the CTV (internal margin) and setup uncertainties (setup margin) in the patient's position relative to the beam. For this study, it was assumed that the location of the PTV is adequately represented by bony structures, due to the anatomy in the head and neck region, thus, the internal target motion is considered negligible. Population-based margins were calculated to ensure a minimum dose of 95% to the CTV for 90% of the patients for all of patients based on the equations of van Herk [18] as shown in equations 3.1.

$$1\text{-D population-based margin} = 1.64\sum\nolimits_{pop} + 0.7\sigma_{pop} \qquad (3.1)$$

Where $\sum_{pop}$ and σ_{pop} are defined by Stroom [8], then the calculated CTV-to-PTV margins were compared to a value 5-10mm based on traditional margins used in King Chulalongkorn Memorial Hospital.

3.8 Outcome to be Measured

3.8.1 Main outcome: The primary outcome is setup variation, measured in random error and systematic error.

3.8.2 Secondary outcome: The secondary outcome is adequate treatment CTV-to-PTV margins.

3.9 Measurement

Outcome variable
- Isocentric deviation
- Individual-based random error
- Population-based random error
- Individual-based systematic error
- Population-based systematic error

3.10 Data Collection

The setup variation, measured in random error and systematic error are calculated by isocentric deviation read out by VARiSVision software.

3.11 Data Analysis

3.11.1 Summarization of data

The setup variation is continuous data. The average and SD are analyzed.

3.11.2 Data presentation

The table and bar chart were presented. CRFs are shown in appendix B.

3.11.3 Statistical evaluation

This study is done to determine the setup variation, measured in random error and systematic error. Statistic evaluation is commenced with the use of Microsoft Excel program for the calculation of the average and standard deviation of parameter in each patient.

3.12 Expected benefit and application

The data will be able to define adequate CTV-to-PTV margin in IMRT of head and neck cancer in Division of Radiation Oncology at King Chulalongkorn Memorial Hospital.

3.13 Ethic consideration

This study was performed on the routine clinical study that the intervention will not directly be operated to the patient during treatment. However, the proposal was approved by the Ethics Committee of Faculty of Medicine, Chulalongkorn University. Consent form and patient information sheet are shown in appendix A.

CHAPTER 4

RESULTS

4.1 Quality control

4.1.1 Quality check of EPID (Contrast detail resolution) using PortalVision ATP phantom.

The contrast detail resolution of EPID was performed on 6 MU and 10 MU for 6 MV photon beam. The results of contrast resolution check are shown in Table 4.1 and Table 4.2. The results of contrast resolution check were in acceptable specification both of 6 MU and 10 MU which an object contrast ≥ 0.2 % were visible.

Table 4.1 Contrast resolution results for aS500 with the PortalVision phantom at isocenter, for an image minimum dose per frame of 6 MU at 6 MV and 10 frames (high quality) with the detector at 140 cm.

Contrast Resolution check	
Test Patient	ZZ-ATP
Specification	
Photon Energy	6 MV (Low-X)
Dose	6 MU (Rep Rate: 1)
Acqu.Quality	High
Actual	⊗ Mark visible holes on image below

Image ID	Low X RR1-1-3
File	

Table 4.2 Contrast resolution results for aS500 with the PortalVision phantom at isocenter, for an image minimum dose per frame of 10 MU at 6 MV and 10 frames (high quality) with the detector at 140 cm.

Contrast Resolution check	
Test Patient	ZZ-ATP
Specification	
Photon Energy	6 MV (Low-X)
Dose	10 MU (Rep Rate: 3)
Acqu.Quality	High
Actual	⊗ Mark visible holes on image below

Image ID	Low X RR1-1-3
File	

4.1.2 Accuracy check of software by using the perspex (PMMA) phantom.

The analyzed images in lateral field and anterior field for image from (left) simulator image and (right) portal image are shown in Figure 4.1 and Figure 4.2. The accuracy of registration software ranged from 0 mm to 0.5 mm. The results were in acceptable range [10].
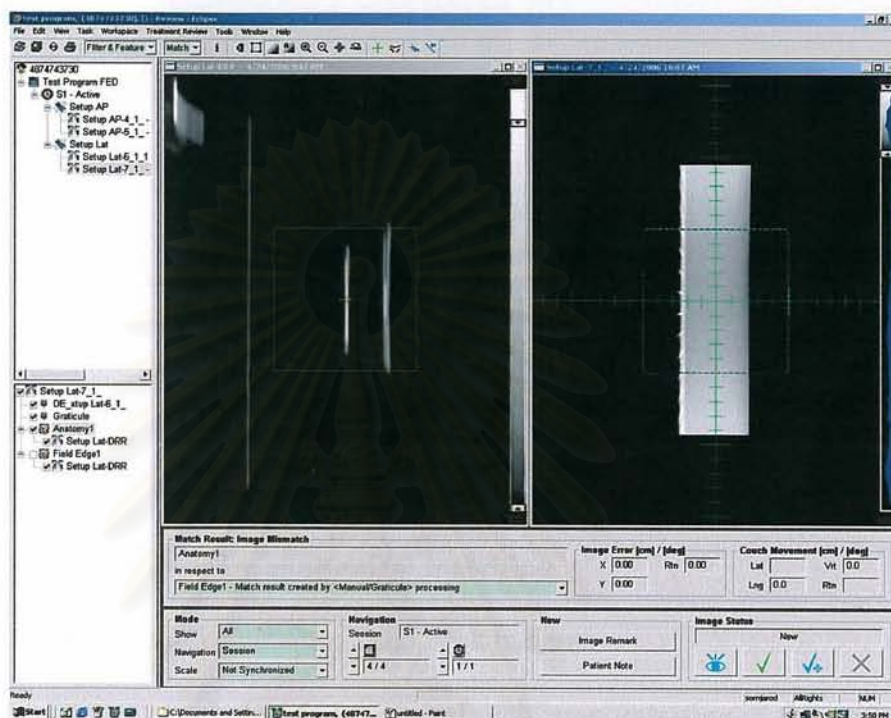
Figure 4.1 Analyzed image: (left) simulator image and (right) portal image in lateral field.
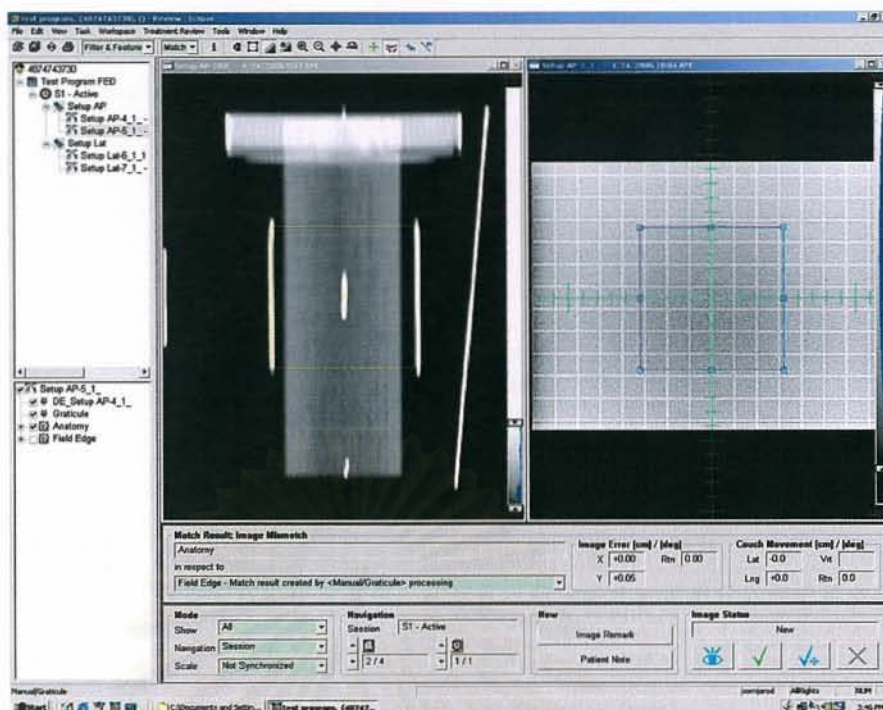
Figure 4.2 Analyzed image: (left) simulator image and (right) portal image in anterior field.

4.2 Portal image analysis by anatomical matching

4.2.1 Setup error for nine head and neck patients

The anatomy matches were performed with superimposing of the portal image and reference image from simulator, the image mismatch were recorded as the coordinates X, Y and Z. The image mismatch which was the interfractional setup errors were analyzed by comparing a total of 168 images (27 simulation images and 141 portal images) and 564 anatomical matches. The results of the isocentric deviation on each anatomical match point of all patients are shown in appendix C.

Since, deviations of the coordinates in the S-I direction were measured on both lateral and AP films, a larger deviation was adopted from a large number of data measurement which was a representative error for the bony landmarks. Positive values in the lateral, A-P and S-I direction represented deviations in the anterior, left and inferior direction of the patients.

The distribution of the interfraction setup errors of each anatomical landmark on both lateral and anterior field are shown in graphically in Figure 4.3 (a) - (b) and Figure 4.4 (a) - (b), respectively. For lateral field, the maximum frequency was occurred at the deviation of -2.0 to -2.5 mm (skull bones), whereas it was 1.0 to 1.5mm (C1) in S-I directionFor anterior fields, the maximum frequency was occurred at the deviation of -0.5 to 0 mm (mandible) in L-R direction whereas it was 0 to 0.5 mm (spinous process) in S-I direction.

Regarding the setup error for lateral field, 78% was within 3mm and 95% was within 5 mm along A-P direction; while 88% was within 3mm and 100% was within 5 mm along S-I direction, respectively. For anterior field, the setup errors were 77% within 3mm, 93% within 5 mm along L-R direction and 74% within 3mm, 95% within 5 mm along S-I direction.
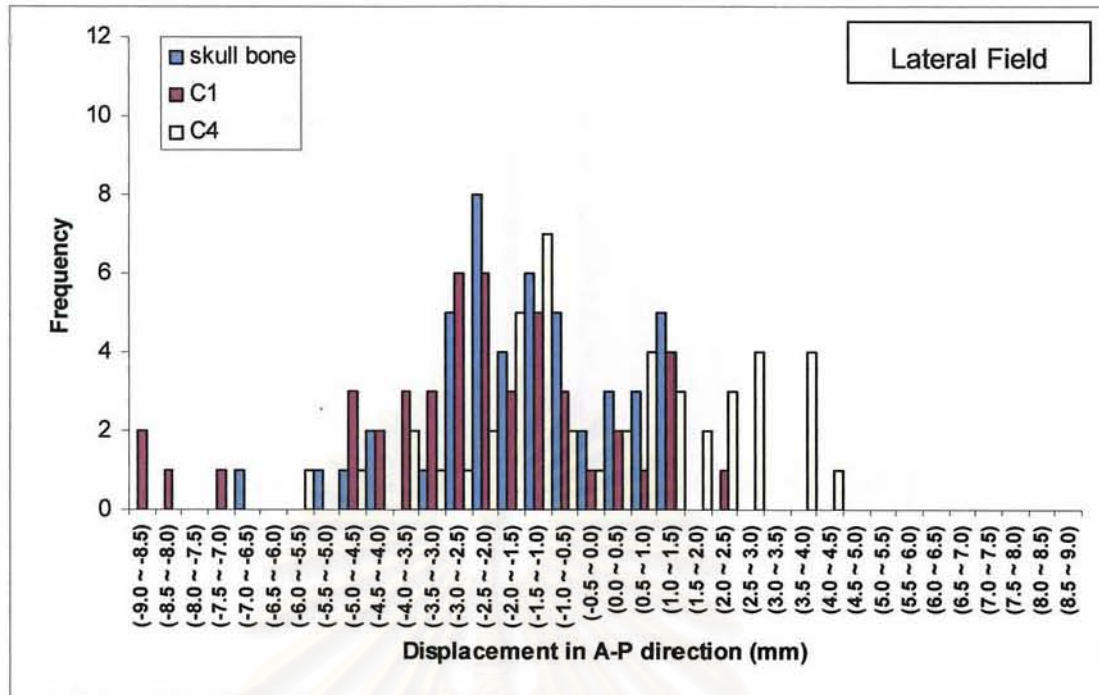
(a)
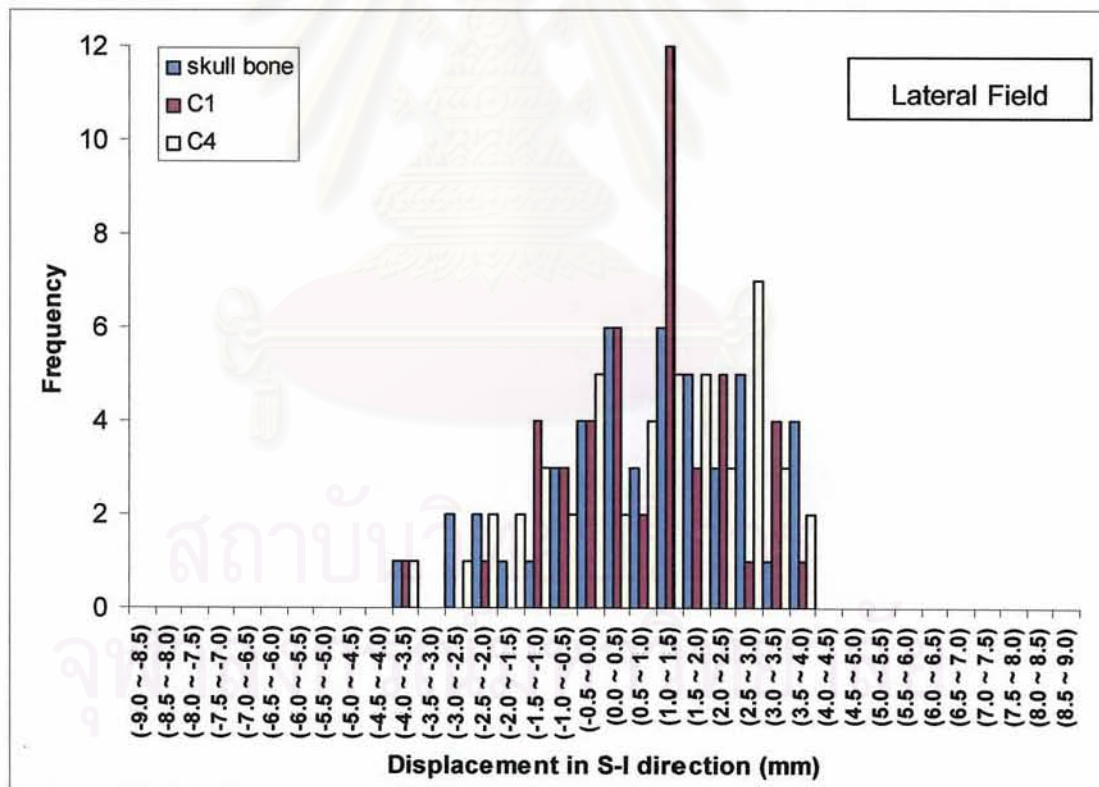
(b)

Figure 4.3 The distribution of the interfraction set up errors of lateral field. The displacements of coordinate between portal images and simulation images are plotted for the (a) Anterior-Posterior (A-P) direction and (b) Superior-Inferior (S-I) direction.
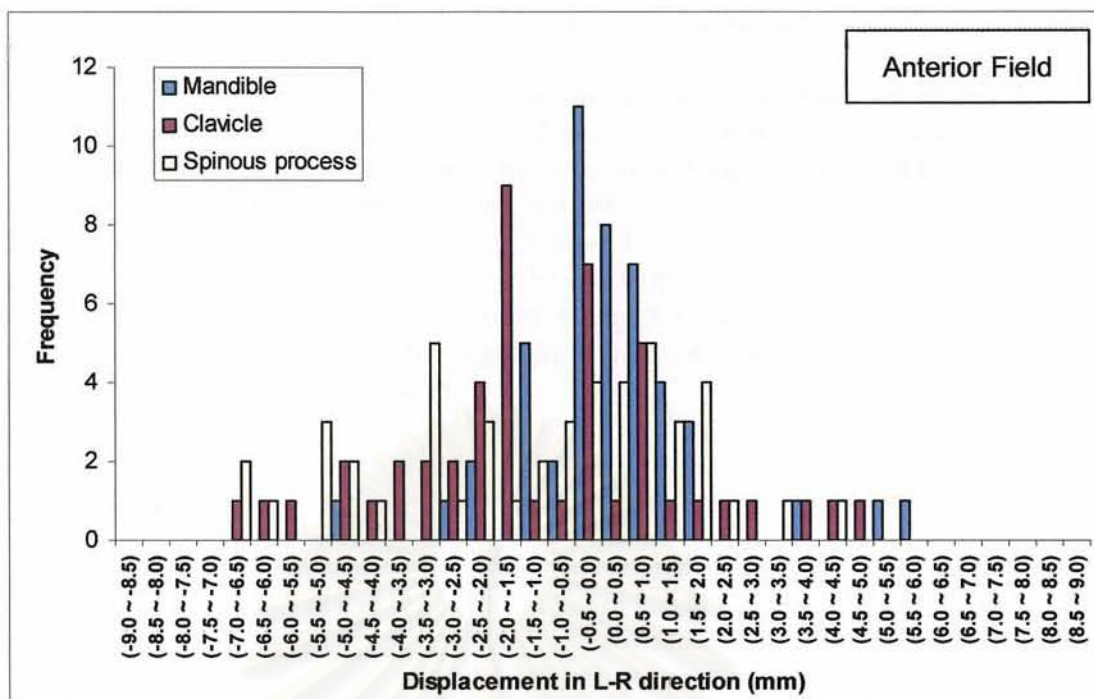
(a)
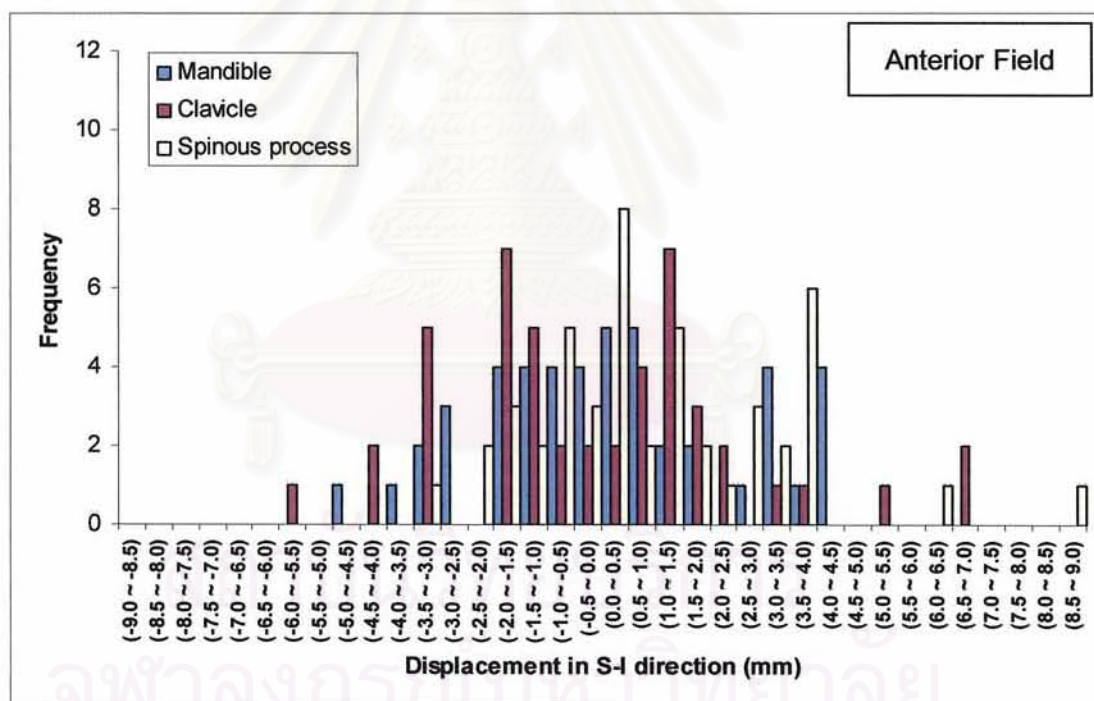
(b)

Figure 4.4 The distribution of the interfraction set up errors of anterior field. The displacements of coordinate between portal images and simulation images are plotted for the (a) Left-Right (L-R) direction and (b) Superior-Inferior (S-I) direction.

4.2.2 Systematic error and random error for individual patient and population

The summary of individual systematic error (Σ_{ind}) and individual random error (σ_{ind}) for the six bony landmarks of lateral and anterior field are presented in Table 4.3 and Table 4.4. The individual systematic error of lateral field ranged from -7.4 to 2.5 mm and -1.9 to 3.4mm along A-P and S-I direction, respectively. For anterior field, the individual systematic error ranged from -4.8 to 2.9 mm and -2.8 to 4.5 along L-R and S-I direction, respectively. The individual random error in lateral field ranged from 0.3 to 3.5 mm and 0.6 to 2.7mm along A-P and S-I direction, respectively. While in the anterior field, they ranged from 0.3 to 4.8 mm and 0.4 to 4.1 mm along L-R and S-I direction, respectively.

Table 4.3 Individual -based statistics (Σ_{ind} and σ_{ind}) calculated for each anatomical structure of all patients along the A-P and S-I axes for lateral field.

Lateral field Pt.No.	Skull bone				C1				C4			
	ΔAP (mm)		ΔSI (mm)		ΔAP (mm)		ΔSI (mm)		ΔAP (mm)		ΔSI (mm)	
	Σ_{ind}	σ_{ind}	Σ_{ind}	σ_{ind}	Σ_{ind}	σ_{ind}	Σ_{ind}	σ_{ind}	Σ_{ind}	σ_{ind}	Σ_{ind}	σ_{ind}
1	-2.7	0.3	2.0	0.9	-3.5	0.8	1.6	0.8	-3.8	1.0	2.2	0.7
2	-0.1	1.7	3.4	0.6	0.5	1.3	2.7	1.2	0.4	1.5	2.4	0.9
3	-5.1	1.0	-0.3	2.7	-7.4	1.8	-1.2	2.2	-0.7	3.1	-0.7	2.1
4	-1.6	0.4	0.2	0.7	-2.0	0.8	0.2	1.1	-1.6	0.4	0.9	0.7
5	-0.4	1.1	0.7	1.6	-2.0	1.0	0.8	1.8	-0.7	0.7	0.9	2.4
6	0.4	0.9	-1.0	2.0	-0.1	2.4	0.4	1.1	2.5	1.8	-0.5	2.3
7	-1.0	1.6	2.0	1.0	-1.8	1.2	1.5	1.2	1.5	1.8	0.9	2.3
8	-1.3	1.0	-1.9	0.8	-2.2	1.8	0.5	0.6	2.0	3.5	-1.4	1.8
9	-1.9	0.8	1.4	0.8	-3.1	1.1	1.2	1.5	0.4	1.7	1.3	1.5

Table 4.4 Individual -based statistics (Σ_{ind} and σ_{ind}) calculated for each anatomical structure of all patients along the L-R and S-I axes for anterior field.

Anterior field	Mandible				Clavicle				Spinous process			
	ΔLR (mm)		ΔSI (mm)		ΔLR (mm)		ΔSI (mm)		ΔLR (mm)		ΔSI (mm)	
Pt.No.	Σ_{ind}	σ_{ind}	Σ_{ind}	σ_{ind}	Σ_{ind}	σ_{ind}	Σ_{ind}	σ_{ind}	Σ_{ind}	σ_{ind}	Σ_{ind}	σ_{ind}
1	0.7	0.9	-0.4	2.3	-1.3	3	-0.4	1.5	-2.5	2.3	1.1	2.9
2	-0.4	1.0	2.9	0.5	-1.5	2.1	4.5	2.5	-0.8	0.9	2.7	0.9
3	1.6	4.8	-2.8	1.7	-2.1	0.3	1.5	0.7	-3.7	2.5	3.7	4.1
4	0.6	1.0	-1.0	0.8	-0.9	0.9	-1.5	1.5	0.4	0.9	-0.7	0.7
5	0.0	0.4	2.1	2.4	-0.9	1.2	-1.2	1.3	-0.7	2.3	1.7	1.6
6	-1.4	1.4	-1.7	1.2	-4.8	1.4	-1.4	3.2	2.4	1.1	-0.8	1.9
7	0.2	0.6	0.2	2.3	-0.8	3.5	-1.3	2.3	-3.3	2.0	0.7	1.9
8	-0.9	0.7	-1.8	0.9	2.9	2.1	1	0.4	0.1	0.9	-1.0	1.0
9	-0.6	0.4	-0.5	1.2	-1.9	2.4	-1.1	4.1	-3.7	2.6	1.3	0.9

The histogram of individual systematic error (Σ_{ind}) and individual random error (σ_{ind}) per patient in lateral and anterior fields in each direction are shown in Figure 4.5 (a) - (d) and Figure 4.6 (e) - (h).

(a)

(b)
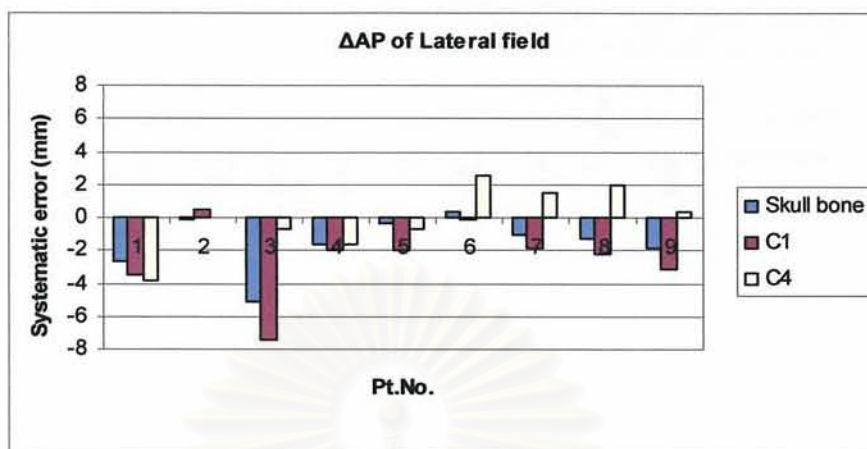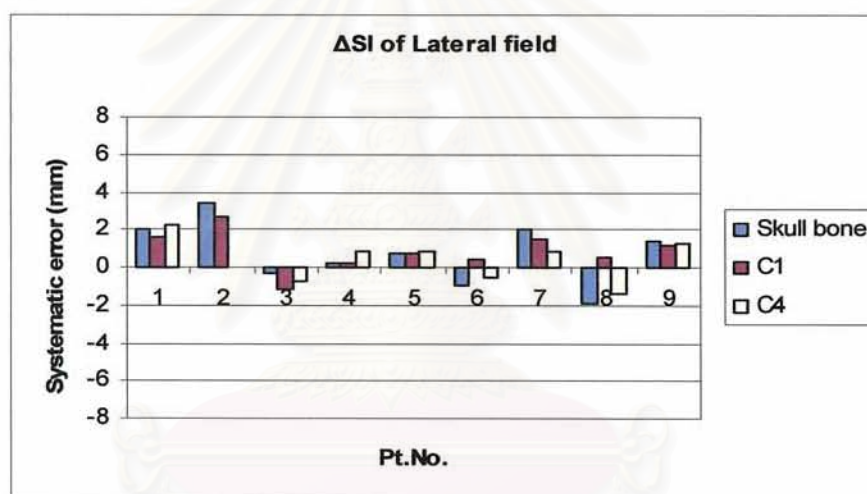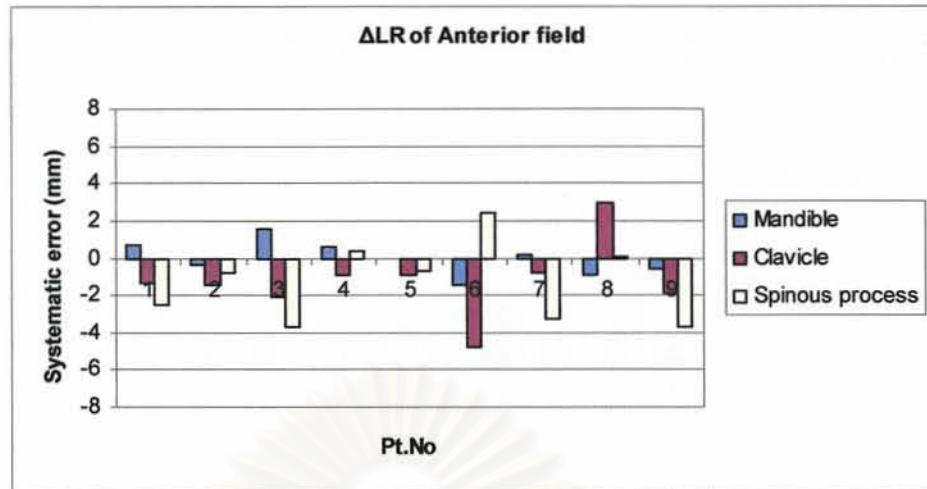
(c)
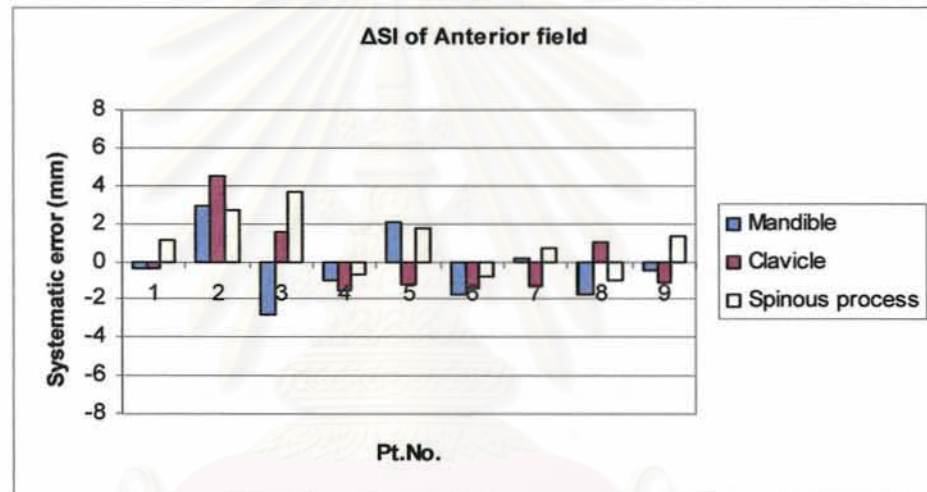
(d)

Figure 4.5 Graphs depicting the individual systematic error (Σ_{ind}) in (a) A-P and (b) S-I direction of lateral field and (c) L-R and (d) S-I direction of anterior field.

(e)

(f)
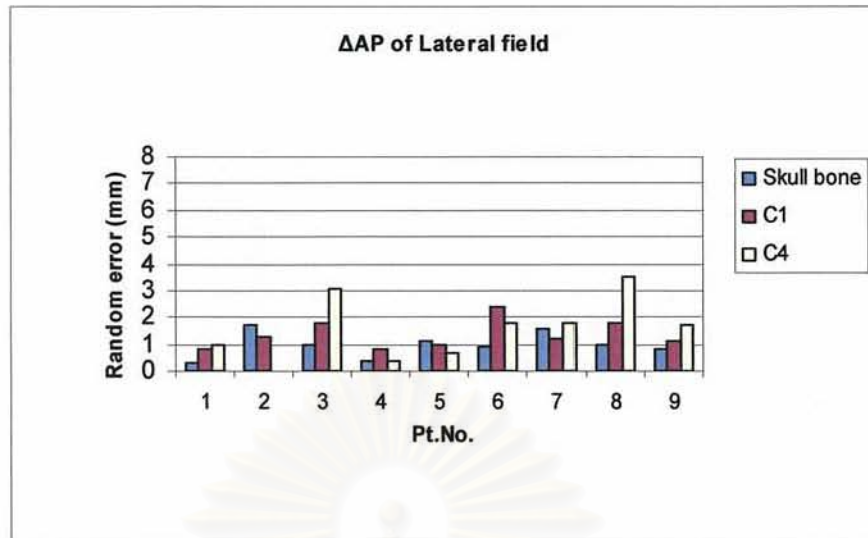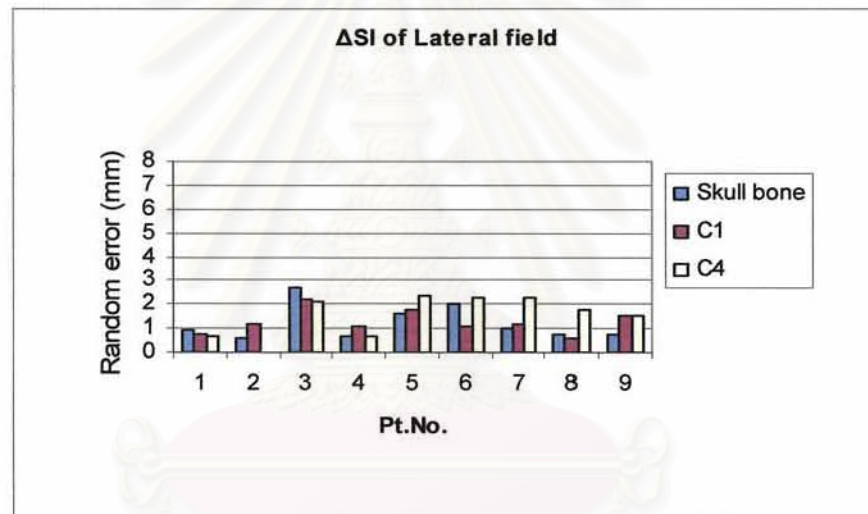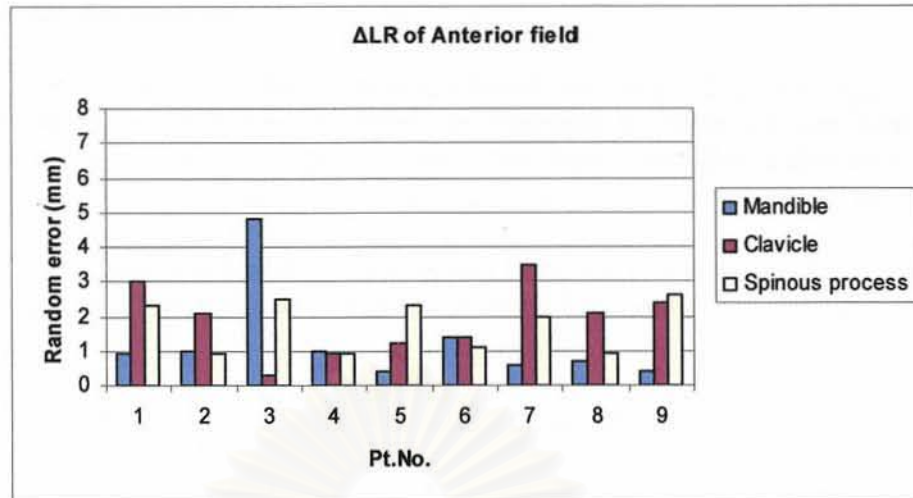
(g)
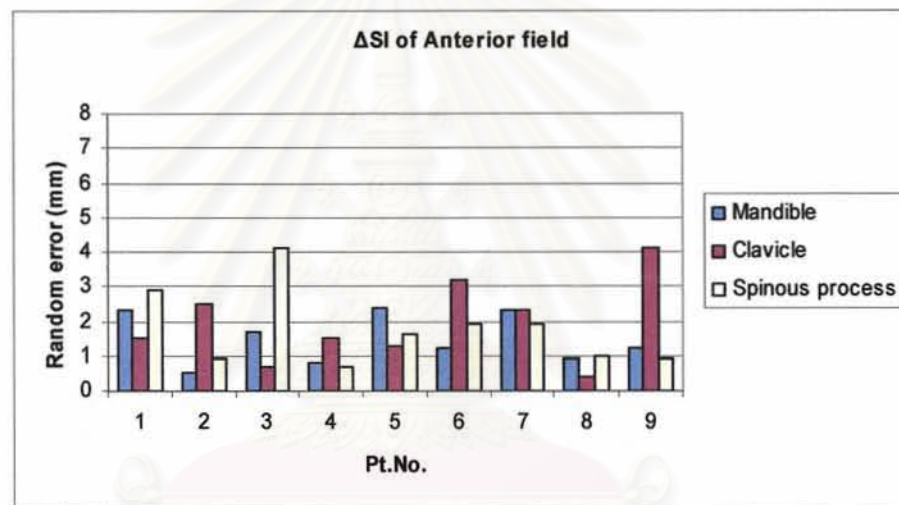
(h)

Figure 4.6 Graphs depicting the individual random error (σ_{ind}) in (e) A-P and (f) S-I direction of lateral field and (g) L-R and (h) S-I direction of anterior field.

4.3 Margin calculation

The summary of the population-based statistics (Σ_{pop} and σ_{pop}) and one-dimensional population-based margins are presented in Table 4.5 and Table 4.6 and the histogram of one-dimensional population-based margins calculated for each anatomical structure of all patients along all axes for anterior field are shown in Figure 4.7 and Figure 4.8.

The population-based margin ranged from 2.4 to 4.9mm (L-R), 3.9 to 5.0mm (S-I) for anterior field and 3.4 to 4.7mm (A-P), 2.7 to 3.6mm (S-I) for the lateral field.

Table 4.5 Population-based statistics (Σ_{pop} and σ_{pop}) and one-dimensional population-based margins ($1.64\Sigma_{pop} + 0.7\sigma_{pop}$) calculated for each anatomical structure of all patients along the A-P and S-I axes for lateral field.

Lateral Field	Skull bone		C1		C4	
	ΔAP(mm)	ΔSI (mm)	ΔAP(mm)	ΔSI (mm)	ΔAP(mm)	ΔSI (mm)
Σ_{pop}	1.6	1.7	2.3	1.1	2.1	1.2
σ_{pop}	1.0	1.2	1.4	1.3	1.8	1.7
Margins	3.4	3.6	4.7	2.7	4.7	3.2

Table 4.6 Population-based statistics (Σpop and σpop) and one-dimensional population-based margins ($1.64\Sigma_{pop} + 0.7\sigma_{pop}$) calculated for each anatomical structure of all patients along the L-R and S-I axes for anterior field.

Anterior Field	Mandible		Clavicle		Spinous process	
	ΔLR(mm)	ΔSI (mm)	ΔLR(mm)	ΔSI (mm)	ΔLR(mm)	ΔSI (mm)
Σ_{pop}	0.9	1.8	2.0	2.0	2.1	1.6
σ_{pop}	1.2	1.5	2.4	2.5	1.7	1.8
Margins	2.4	4.1	4.9	5.0	4.7	3.9
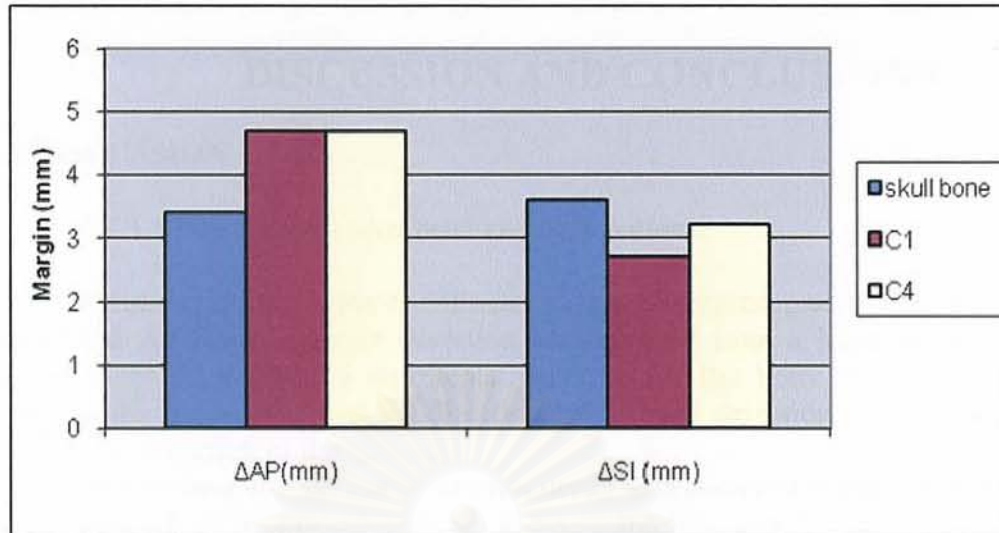
Figure 4.7 Graphs depicting the one-dimensional population-based margins of lateral field in A-P and S-I direction.
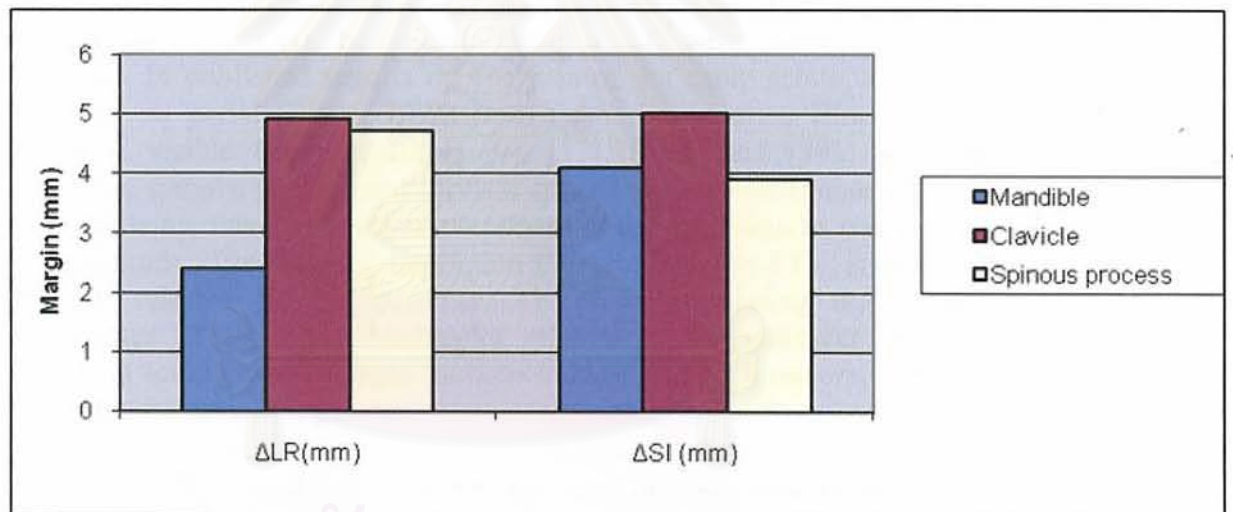
Figure 4.8 Graphs depicting the one-dimensional population-based margins of anterior field in L-R and S-I direction.

CHAPTER 5

DISCUSSION AND CONCLUSIONS

5.1 DISCUSSION

5.1.1 Setup error for nine head and neck patients

Since deviations of the coordinates in the S-I direction were measured on both lateral and AP films, a larger deviation was adopted from a large number of data measurement which was a representative error for the bony landmarks. Positive values in the lateral, A-P and S-I direction represented deviations in the anterior, left and inferior direction of the patients.

In A-P direction the maximum frequency was occurred at the deviation of -2.0 to -2.5 mm (skull bones), whereas for the S-I direction was 1.0 to 1.5 mm (C1) for lateral field. For anterior fields, the maximum frequency was occurred at the deviation of -0.5 to 0 mm (mandible) in L-R direction whereas for the S-I direction was 0 to 0.5 mm (spinous process).

In the present study, the interfractional displacements of the six bony landmarks, not the treatment isocenter, were analyzed. The magnitudes of the interfractional errors were quantified by measuring the displacements of the coordinates of the six bony landmarks, which were determined relative to the isocenter. In published reports on analyses of the setup errors, displacement of the isocenter on portal film or EPID from that on simulation films was measured by matching visible bony structures [9], [17], [119] and [20]. Since the clavicle, mandible, spinous process and cervical spine can move independently with breathing or swallowing, interfractional displacement of these landmarks was expected to differ in magnitude. The dose of irradiation delivered to the PTV is determined by the position relative to the isocenter. Therefore, measuring the deviation of the coordinates of the bony landmarks relative to the isocenter is appropriate for analyzing setup errors or organ motions in head and neck tumors, which are expected to move with underlying bone.

5.1.2 Systematic error and random error for individual patient and population

Systematic error can arise from various factors, the most important being transfer errors from simulator to the treatment unit. Random errors are related to any accidental error during setup, due to mispositioning of the patient in the mask, movements of the patient or organ motion in the period between positioning and start of irradiation or during irradiation.

The setup errors in term of systematic and random error were evaluated. The error was measured on a weekly basis for a number of patients and fractions. To calculated setup error for individual patient, the systematic and random errors were calculated according to equation (2.1) and (2.2).

The maximum shift was 7.4 mm in the posterior direction for individual systematic error, while it was 4.8mm to the right direction for individual random error. The possible explanation for such a big deviation, although in only small number of patients was the decreased sign of neck nodes from radiation treatment which resulted in loosening of the mask. Re-do of immobilization mask might solve

this problem, but with the trade-off when the new CTV and PTV need to be re-delineated.

The systematic errors were much larger than the random errors. Large systematic errors lead to large underdosage for some of the patients, while large random errors lead to a moderate underdosage for a large number of patients. The systematic error was due to the treatment preparation error, which frequently occurs in the transfer of information from the simulator to the treatment unit. Such errors could be due to discrepancies between the couch top, the laser alignment system, or cross hair alignment. There were many variables, other than immobilization devices, that affect the setup accuracy, including patient comfort and cooperation, reliance on skin marking, equipment uncertainties, and the attentiveness of the technologist when setup the treatment.

Prisciandaro et al. [9] reported that systematic errors ranged from -0.3 to -0.2 mm, -0.2 to 1.1 mm and -0.4 to 1.2 mm and random errors ranged from 3.0 to 3.6 mm, 2.2 to 3.3 mm and 2.6 to 2.7 mm, along the L–R, S–I and A–P axes, respectively, using TYPE-S^{TM} head/neck shoulder immobilization systems. While our study, using the same type immobilization system, showed that systematic errors ranged from -3.5 to 2.9mm, -2.8 to -4.5mm and -7.4 to 2.5mm and random errors ranged from 0.4 to 4.8mm, 0.4 to 3.8mm and 0.2 to 3.1mm along the L-R, S-I and A-P axes, respectively. Although systematic errors in our study exceeded those in previous work, the random errors were comparable.

Prisciandaro yielded smaller systematic errors with a thermoplastic mask covering head compared with mask covered face alone, so rigorous immobilization devices such as the head, neck and shoulder immobilization shell might be prerequisite for highly conformal radiotherapy such as IMRT or 3D conformal radiotherapy for head and neck tumors. Thus our immobilization device was suitable for treatment setup.

5.1.3 Margin calculation

The result showed the population-based margin ranged from 2.4 to 4.9mm (L-R), 3.9 to 5.0mm (S-I) for anterior field and 3.4 to 4.7mm (A-P), 2.7 to 3.6mm (S-I) for the lateral field.

Consider margin along S-I axis which was the co-axis both in anterior field and lateral field, the difference in one-dimensional population-based margins along S-I axis between anterior field (3.9 to 5.0 mm) and lateral field (2.6 to 3.7mm) were observed because the clavicles chosen for anterior field at the shoulder level were less stable than anatomical landmarks chosen for lateral field i.e. skull bones, C1 and C4. However, the margin calculated from various anatomical structures and for each axis had a wide range of margin, the large difference of the margins was occurred because of difference of stability in each bony landmark selected as a reference.

According to ICRU Report 62, [1] setup and organ positional uncertainties should be incorporated into the treatment planning process by taking a margin around the CTV, thereby defining the PTV. How these margins should be defined as a function of the distribution of organ position and setup errors was not specified. In this study, 1-dimensional population-based margins were calculated for all of patients based on the equations of van Herk [18] according to equation (3.1). The result showed the population-based margin ranged from 2.4 to 5.0mm. Based on the dose population histograms, they derived a margin recipe to guarantee that 90% of patients in the population receive a minimum cumulative CTV dose of at least 95% of the

prescribed dose. This margin is approximately $2.15\Sigma + 0.7\sigma$ for 2-dimentional population-based margins, whereas approximately $2.5\Sigma + 0.7\sigma$ for 3-dimentional population-based margins. Based on these equations, the 2-dimentional population-based margins and 3-dimentional population-based margins ranged from 2.8mm to 6.1mm (22% discrepancy from 1-dimentional margin) and 3.2mm to 6.8mm (36% discrepancy), respectively.

Stroom et al. [8] developed a different method for calculation of CTV-to-PTV margin for a prostate, cervix and lung cancer cases which ensures at least 95% dose to 99% of the CTV. It appears to be equal to about $2\Sigma + 0.7\sigma$ for three all cases, based on assumption that the CTV should be adequately irradiated with a high probability. A fundamental problem of coverage probabilities is that they tend to undervalue sharp tumor extensions, which are smeared out to very low probability levels and will not be included in the margin. In clinical practice one might prefer a tighter CTV-to-PTV margin near a dose-limiting structure. Based on result in our study, we found that the population-based margin ranging from 3.1mm to 5.8mm (16% discrepancy), when calculated population-based margin according to equation of Stroom [8].

As seen from the calculated margin above, there is some among between 1-dimentional, 2-dimentional, 3-dimentional margin and margin that derive from other author [8]. Although the SD of different geometrical errors should be added in quadrature, random and systematic often result in different margins, and how these should be added may not always be clear. The simplest situation is when the margin is defined as a probability level of the minimum dose. In that case, the PTV margin is generated using a first margin for systematic errors that ensures certain percentage coverage, followed by adding a margin for random errors that ensures coverage of the first margin up to a given dose. However, such a linear addition of margins is not valid for margins based on probabilities and/or biological effects. When margins are defined based on probability levels, they should be added in quadrature because the margins represent the width of probability distributions. Similarly, one may expect an interaction between CTV and PTV margins when both are based on probability levels. Such an interaction has, however, not yet been investigated.

Ideally, the CTV-to-PTV margin should be determined solely by the magnitudes of the uncertainties involved. In practice, the clinician usually also considers to abutting healthy tissues when deciding on the size of the CTV-to-PTV margin [11]. However, it should be noted that the larger margins leading to higher dose to the critical normal structure whereas the smaller margins leading to risk of missing the target. For instance, a zero margin at one side of the tumor will lead to a very high change that part of the tumor there is underdosed. Thus, to ensure the optimum margin, should be weighed against the risk and benefit to each individual patients.

Setup uncertainties are not the only margins to be included in the PTV which should also include a security margin for organ motions. However, in setting of the PTV-margins for head and neck tumors, the management of the organ motions is a subject of controversy. Gieleau et al. [17] claimed that the intrafractional organ motions of head and neck tumors could be neglected for calculating the PTV-margin since the values were trivial. Hamlet [21] studied the larynx motions during normal breathing and swallowing and demonstrated no significant impact on dose distribution. In present study, population-based margins were calculated for all of patients based on the equations of van Herk [18] that suggested a one-dimensional margin of $1.64\Sigma_{pop} + 0.7\sigma_{pop}$ to ensure a minimum dose of 95% to the CTV for 90% of the patients. In this study, population-based margins ranged from 2.4 to 5.0 mm

were demonstrated, which were comparable to our traditional margin of 5mm in our department. It seems that we can further decrease CTV-to-PTV margin to spare more organ-at-risk in the future.

5.2 CONCLUSIONS

The primary objective of the present study was to measure interfraction setup variation in nine head and neck cancer patients undergoing IMRT with 6MV X-ray beam from Clinac23EX using an EPID. Before collecting the patient data, the quality control of EPID and image software had been performed to verify the accuracy of the images.

In our study, to determine interfraction setup variation, the simulator images were used as the reference to which the portal images were compared. The results showed individual systematic error (Σ_{ind}) ranged from -4.8 to 2.9 mm, -2.8 to 4.5 mm and -7.4 to 2.5 mm along L-R, S-I and A-P direction, respectively, while the corresponding individual random error (σ_{ind}) ranged from 0.3 to 4.8 mm, 0.4 to 4.1 mm and 0.3 to 3.5 mm along the L-R, S-I and A-P axes. The results of interfraction setup variation showed that the shifts were predominantly in posterior, right and inferior directions.

The secondary objective of the present study was to define adequate CTV-to-PTV margin for IMRT of head and neck cancer in our department.

The size of a margin between the CTV and PTV is a balance between the targeting accuracy and dose constraints on tumor and normal tissue. The margin should be sufficient to account for all geometric errors such that the CTV accumulates no less than, 95% of the prescribed dose. Various factors have been included in the statistical techniques for manufacturing a suitable margin. The degree of interfraction setup variation is a vital parameter for the assessment of population-based margin calculations. Although several authors have provided suggestions for necessary margins, based on population-based studies, the true extent of CTV-to-PTV margins is institute specific. The results of this study suggested that the determination of setup variation is important for assessment of population-based margin calculation to achieve adequate CTV-to-PTV margin of head and neck cancer patient.

The population-based margin ranged from 2.4 to 4.9mm (L-R), 3.9 to 5.0mm (S-I) for anterior field and 3.4 to 4.7mm (A-P), 2.7 to 3.6mm (S-I) for the lateral field. These margins were less than the margin that prescribed at our department (5 – 10 mm) for head and neck cancer. Moreover, 79% of all displacements were within 3mm and 96% were within 5 mm. Thus the current margin provided sufficient coverage for all of the patients.

REFERENCES

1. International Commission on Radiation Units and Measurements, "ICRU Report 62: Prescribing, Recording and Reporting Photon Beam Therapy (Supplement to ICRU Report 50)" (1999).
2. Eisbruch A, Chao KS and Garden A. "Phase I/II study of conformal and intensity modulated irradiation for oropharyngealcancer, RTOG H-0022, "AvailableOnline:http://rtog.org/members/protocols/h0022/h0022.pdf (2001).
3. Head and neck cancer ; http://www.oncologychannel.com/**headneck/**
4. Cancer in Thailand ; http://www.nci.go.th/cancer_record/index.htm
5. Eisbruch A. Head and neck cancer In: Arno JM and John CR, *Intensity-Modulated Radiation Therapy: A clinical perspective*. London: Bc Decker Inc; 2005. p. 264-75.
6. Chao KS and Blanco AI. Intensity-Modulated Radiation Therapy For Head And Neck Cancer. In: Samual H. *A practical guide to intensity-modulated radiation therapy*. Madison WI: Medical Physics Publishing; 2003. p. 631-40
7. Balter J .Target and Critical Structure Definitions, Dose Prescription, and Reporting for IMRT. In: Keall P, Wu Q, Wu Y, et al. *Intensity-Modulated Radiation Therapy. The state of the art* .Madison WI: Medical Physics Publishing; 2003. p. 183-95.
8. Stroom JC and Heijmen Ben JM. Geometrical uncertainties, radiotherapy planning margins, and the ICRU-62 report. *Radiother Oncol* 2002; 64: 75-83.
9. Prisciandaro JI, Frechette CM, Herman MG, et al. A methodology to determine margins by EPID measurements of patient setup variation and motion as applied to immobilization devices. *Med Phys* 2004; 31: 2978–88.
10. Langmack KA. Portal imaging. *Br J Radiol* 2001; 74: 789-804.
11. Xia P and Chuang C. Patient-Specific Quality Assurance in IMRT. In: Samual H. *A practical guide to intensity-modulated radiation therapy*. Madison WI: Medical Physics Publishing; 2003. p. 495-513
12. Xing L, Lin Z, Donaldson SS, et al. Dosimetric effects of patient displacement and collimator and gantry angle misalignment on intensity modulated radiation therapy. *Radiother Oncol* 2000; 56: 97–108.
13. Manning MA, Wu Q, Cardinale RM, et al.The effect of setup uncertainty on normal tissue sparing with IMRT for head-and-neck cancer. *Int J Radiat Oncol Biol Phys* 2001; 51: 1400–9.
14. Hurkmans CW, Remeijer P, Lebesque J V, et al. Set-up verification using portal imaging; review of current clinical practice. *Radiother Oncol* 2001; 58:105–20.
15. Hess CF, Kortmann RD, Jany R, et al. Accuracy of field alignment in radiotherapy of head and neck cancer utilizing individualized face mask immobilization: a retrospective analysis of clinical practice. *Radiother Oncol* 1995; 34:69-72.
16. Huizenga H, Levendag PC, De Porre PM, et al. Accuracy of radiation field alignment in the head and neck cancer: a prospective study. *Radiother Oncol* 1988; 81:181–7.
17. Gilbeau L, Octave-Prignot M, Loncol T, et al. Comparison of setup accuracy of three different thermoplastic masks for the treatment of brain and head and neck tumors. Radiother Oncol 2001; 58: 155–62.

18. van Herk M, Remeijer P, Rasch C, et al. The probability of correct target dosage: dose–population histograms for deriving treatment margins in radiotherapy. *Int J Radiat Oncol Biol Phy* 2000; 47: 1121–35.

19. Bel A, Keus R, Vijlbrief RE, et al. Setup deviations in wedged pair irradiation of parotid gland and tonsillar tumors, measured with an electronic portal imaging device. *Radiother Oncol* 1995; 37: 153–9.

20. de Boer HC, van Sörnsen de Koste J., Creutzberg CL, et al. Electronic portal image assisted reduction of systematic set-up errors in head and neck irradiation. *Radiother Oncol* 2001; 61: 299–308.

21. Hamlet S, Ezzell G and Aref A. Larynx motion associated with swallowing during radiation therapy. *Int J Radiat Oncol Biol Phys* 1994; 28: 467-70.

APPENDICES

APPENDIX A

ข้อมูลสำหรับผู้เข้าร่วมการวิจัย (Patient Information)

การศึกษา : การวัดความคลาดเคลื่อนของตำแหน่งการฉายรังสีในผู้ป่วยมะเร็งศีรษะและลำคอ ที่รักษาด้วยเทคนิคฉายรังสีแบบปรับความเข้ม โดยใช้เครื่องถ่ายภาพทางรังสีแบบตัวเลข

เรียน ผู้เข้าร่วมการวิจัยทุกท่าน

ท่านเป็นผู้ได้รับเชิญจากผู้วิจัยให้เข้าร่วมการศึกษาเพื่อวัดความคลาดเคลื่อนของตำแหน่งการฉายรังสีในผู้ป่วยมะเร็งศีรษะและลำคอ ที่รักษาด้วยเทคนิคฉายรังสีแบบปรับความเข้ม โดยใช้เครื่องถ่ายภาพทางรังสีแบบตัวเลข ก่อนที่ท่านตกลงเข้าร่วมการศึกษาดังกล่าว ขอเรียนให้ท่านทราบถึงเหตุผลและรายละเอียดของการศึกษาวิจัย ในครั้งนี้

การรักษาผู้ป่วยมะเร็งศีรษะและลำคอด้วยเทคนิคฉายรังสีแบบปรับความเข้มนั้น ใช้ลำรังสีคลุมเฉพาะขอบเขตของก้อนมะเร็ง หลีกเลี่ยงปริมาณรังสีที่อวัยวะใกล้เคียง อย่างไรก็ตามแพทย์ได้ทำการฉายรังสีที่เผื่อขอบเขตออกไปเล็กน้อย เพื่อป้องกันความคลาดเคลื่อนที่อาจเกิดขึ้นได้จากการจัดท่าผู้ป่วย ดังนั้นการฉายรังสีจึงจำเป็นที่จะต้องถูกต้อง คงที่และแม่นยำ

การศึกษาวิจัยในครั้งนี้ มีวัตถุประสงค์เพื่อ วัดความคลาดเคลื่อนของตำแหน่งการฉายรังสีในผู้ป่วยมะเร็งศีรษะและลำคอ ที่รักษาด้วยเทคนิคฉายรังสีแบบปรับความเข้ม เพื่อดูว่าขอบเขตที่เผื่อไว้เดิมเหมาะสมหรือจะต้องปรับเปลี่ยน

ในการศึกษานี้จะศึกษาโดยการนำภาพจากการถ่ายภาพก่อนการฉายรังสี (Portal image) ที่ถ่ายเพื่อตรวจสอบความถูกต้องในทุกๆสัปดาห์ มาเปรียบเทียบกับภาพที่ได้จากการจำลองการรักษา (Simulation image) ซึ่งใช้เป็นภาพอ้างอิง เพื่อหาความคลาดเคลื่อนของตำแหน่งการฉายรังสี ซึ่งการศึกษานี้เป็นความพยายามเพิ่มคุณภาพและมาตรฐานโดยที่ท่านไม่ต้องเสียค่าใช้จ่ายใดๆ เพิ่มเติมจากการค่ารักษาเดิมของท่านทั้งสิ้น

การเข้าร่วมการศึกษาวิจัยนี้ เป็นไปโดยสมัครใจท่านอาจจะปฏิเสธที่จะเข้าร่วม หรือถอนตัวจากการศึกษาวิจัยนี้ได้ทุกเมื่อโดยไม่กระทบต่อการให้บริการและการรักษาที่ท่านจะได้รับจากนักรังสีการแพทย์ นักฟิสิกส์การแพทย์และรังสีแพทย์หรือผู้ให้บริการท่านอื่นๆ

ประการสำคัญที่ท่านควรทราบ คือ ผลของการศึกษาวิจัยนี้ จะใช้สำหรับวัตถุประสงค์ทางวิชาการเท่านั้น โดยข้อมูลของท่านจะถูกเก็บเป็นความลับ จะไม่มีการเผยแพร่สู่สาธารณชน โดยจะเปิดเผยข้อมูลเป็นภาพรวมในแง่วิชาการเท่านั้น

หากท่านมีปัญหา หรือข้อสงสัยประการใด กรุณาติดต่อ น.ส.นันทพร นัยเนตร
สาขาวิชาฉายาเวชศาสตร์ ภาควิชารังสีวิทยา คณะแพทยศาสตร์ จุฬาลงกรณ์มหาวิทยาลัย
โทร 089 – 5045645 ซึ่งยินดีให้คำตอบแก่ท่านทุกเมื่อ

ขอขอบคุณในความร่วมมือของท่านมา ณ ที่นี้

ใบยินยอมเข้าร่วมการวิจัย (Consent form)

การวิจัย เรื่อง การวัดความคลาดเคลื่อนของตำแหน่งการฉายรังสีในผู้ป่วยมะเร็งศีรษะและลำคอ ที่รักษาด้วยเทคนิคฉายรังสีแบบปรับความเข้ม โดยใช้เครื่องถ่ายภาพทางรังสีแบบตัวเลข

วันให้คำยินยอม วันที่.........................เดือน...............................พ.ศ. ....

ก่อนที่จะลงนามในใบยินยอมให้ทำการวิจัยนี้ ข้าพเจ้าได้รับการอธิบายจากผู้วิจัยถึงวัตถุประสงค์ของการทำวิจัย วิธีการวิจัย อันตรายหรืออาการที่อาจเกิดขึ้นจากการทำวิจัย รวมทั้งประโยชน์ที่จะเกิดขึ้นจากการทำวิจัยอย่างละเอียดและมีความเข้าใจดีแล้ว

ผู้วิจัยรับรองว่าจะตอบคำถามต่างๆ ที่ข้าพเจ้าสงสัยด้วยความเต็มใจไม่ปิดบังซ่อนเร้นจนข้าพเจ้าพอใจ

ข้าพเจ้ามีสิทธิที่จะบอกเลิกการเข้าร่วมในโครงการวิจัยนี้เมื่อใดก็ได้ และเข้าร่วมโครงการวิจัยนี้โดยสมัครใจ และการบอกเลิกการเข้าร่วมการวิจัยนี้ จะไม่มีผลใดๆ ต่อข้าพเจ้า

ผู้วิจัยรับรองว่าจะเก็บข้อมูลเฉพาะเกี่ยวกับตัวข้าพเจ้าเป็นความลับ และจะเปิดเผยได้เฉพาะในรูปที่เป็นสรุปผลการวิจัย การเปิดเผยข้อมูลเกี่ยวกับตัวข้าพเจ้าต่อหน่วยงานต่างๆ ที่เกี่ยวข้องกระทำได้เฉพาะกรณีที่จำเป็น ด้วยเหตุผลทางวิชาการเท่านั้น

ข้าพเจ้าได้อ่านข้อความข้างต้นแล้ว และมีความเข้าใจดีทุกประการ และได้ลงนามในใบยินยอมนี้ด้วยความเต็มใจ

ลงนาม...ผู้ยินยอม

(..)

ลงนาม...พยาน

(..)

ลงนาม...ผู้ทำวิจัย

(..)

APPENDIX B

Case Record Forms

Table I. Spreadsheet for a right lateral field matched over the course of six fractions to skull bones, C1 and C4, respectively. ΔAP and ΔSI represent the deviations in the A-P and S-I direction of each anatomical landmark between simulation images and portal images.

Patient No.		Skull bones		C1		C4	
Date	Fraction	ΔAP (mm)	ΔSI (mm)	ΔAP (mm)	ΔSI (mm)	ΔAP (mm)	ΔSI (mm)
	1						
	2						
	3						
	4						
	5						
	6						
Σ_{ind}							
σ_{ind}							

Table II. Spreadsheets for an anterior field matched over the course of six fractions to mandible, clavicle and spinous process, respectively. ΔLR and ΔSI represent the deviations in the L-R and S-I direction of each anatomical landmark between simulation images and portal images.

Patient No.		Mandible		Clavicle		Spinous process	
Date	Fraction	ΔLR(mm)	ΔSI (mm)	ΔLR(mm)	ΔSI (mm)	ΔLR(mm)	ΔSI (mm)
	1						
	2						
	3						
	4						
	5						
	6						
Σ_{ind}							
σ_{ind}							

APPENDIX C

Data from Individual Nine Patients

Table I. Spreadsheet for a right lateral field matched over the course of six fractions to skull bones, C1 and C4, respectively. ∆AP and ∆SI represent the deviations in the A-P and S-I direction of each anatomical landmark between simulation images and portal images. Positive shifts correspond to anterior and inferior shifts while negative shifts correspond to posterior and superior shifts.

Patient No.1		Skull bones		C1		C4	
Date	Fraction	∆AP (mm)	∆SI (mm)	∆AP (mm)	∆SI (mm)	∆AP (mm)	∆SI (mm)
3/1/2006	1	-3	2.3	-3.5	1.4	-4.9	1.8
3/3/2006	2	-2.7	0.3	-3.7	0.3	-3.7	1.8
3/7/2006	3	-2.4	2.9	-4.8	2.4	-4.8	3.4
3/14/2006	4	-2.9	1.9	-2.4	2.4	-2.4	2.4
3/21/2006	5	-2.9	1.9	-3.9	1.4	-3.9	1.4
3/28/2006	6	-2.4	2.4	-2.9	1.4	-2.9	2.4
Σ_{ind}		-2.7	2.0	-3.5	1.6	-3.8	2.2
σ_{ind}		0.3	0.9	0.8	0.8	1.0	0.7

Patient No. 2		Skull bones		C1		C4	
Date	Fraction	∆AP (mm)	∆SI (mm)	∆AP (mm)	∆SI (mm)	∆AP (mm)	∆SI (mm)
4/25/2006	1	-2.5	3.5	1	3.5	1.3	3
5/2/2006	2	1	3.8	2	3.3	1.5	2.8
5/8/2006	3	1	2.5	-1	1	-1.8	1
5/15/2006	4	0	3.6	0	3	0.5	2.8
Σ_{ind}		-0.1	3.4	0.5	2.7	0.4	2.4
σ_{ind}		1.7	0.6	1.3	1.2	1.5	0.9

Patient No.3		Skull bones		C1		C4	
Date	Fraction	∆AP (mm)	∆SI (mm)	∆AP (mm)	∆SI (mm)	∆AP (mm)	∆SI (mm)
3/8/2006	1	-4.3	-2.9	-4.3	-1	2.4	-1
3/14/2006	2	-5.3	0	-7.2	-0.5	0.5	0
3/20/2006	3	-4.8	0	-8.7	-2.4	-5.8	-0.5
3/27/2006	4	-6.8	-2.4	-8.2	-3.9	0.5	-3.9
3/28/2006	5	-4.3	3.9	-8.7	1.9	-1	1.9
Σ_{ind}		-5.1	-0.3	-7.4	-1.2	-0.7	-0.7
σ_{ind}		1.0	2.7	1.8	2.2	3.1	2.1

Patient No.4		Skull bones		C1		C4	
Date	Fraction	ΔAP (mm)	ΔSI (mm)	ΔAP (mm)	ΔSI (mm)	ΔAP (mm)	ΔSI (mm)
3/22/2006	1	-1.4	-0.8	-1.5	-1	-1.5	0.3
3/23/2006	2	-1.9	1	-1.4	1	-1.4	0.5
3/27/2006	3	-1.4	0	-1.4	-1.4	-1	0.5
4/3/2006	4	-1.1	0	-1.7	0	-1.7	1.7
4/10/2006	5	-2	-0.5	-3	1	-2.3	1
4/18/2006	6	-2	1	-1.5	1.5	-1.5	2
4/24/2006	7	-1.1	0.5	-3.2	0.5	-1.6	0.5
Σ_{ind}		-1.6	0.2	-2.0	0.2	-1.6	0.9
σ_{ind}		0.4	0.7	0.8	1.1	0.4	0.7

Patient No.5		Skull bones		C1		C4	
Date	Fraction	ΔAP (mm)	ΔSI (mm)	ΔAP (mm)	ΔSI (mm)	ΔAP (mm)	ΔSI (mm)
5/26/2006	1	-0.4	-0.9	-2.5	-1.5	-1.5	-2
6/19/2006	2	0.5	3.1	-0.5	3.1	0	3.6
6/26/2006	3	0.6	0.6	-1.7	1.1	-1.1	1.1
7/13/2006	4	-2.2	-0.5	-3.3	-0.5	0	-1.1
7/17/2006	5	-0.6	1.1	-2.2	1.7	-1.1	2.8
Σ_{ind}		-0.4	0.7	-2.0	0.8	-0.7	0.9
σ_{ind}		1.1	1.6	1.0	1.8	0.7	2.4

Patient No.6		Skull bones		C1		C4	
Date	Fraction	ΔAP (mm)	ΔSI (mm)	ΔAP (mm)	ΔSI (mm)	ΔAP (mm)	ΔSI (mm)
7/31/2006	1	1	-1.5	1	0	2.6	-0.5
8/7/2006	2	1.1	1.6	-4.3	1.1	-0.5	3.2
8/21/2006	3	0	-0.5	0.5	2	2.5	-0.5
8/28/2006	4	-1	-0.5	1	-0.5	3.5	-2
9/4/2006	5	1	-3.9	1.4	-0.5	4.3	-2.9
Σ_{ind}		0.4	-1.0	-0.1	0.4	2.5	-0.5
σ_{ind}		0.9	2.0	2.4	1.1	1.8	2.3

Patient No.7		Skull bones		C1		C4	
Date	Fraction	ΔAP (mm)	ΔSI (mm)	ΔAP (mm)	ΔSI (mm)	ΔAP (mm)	ΔSI (mm)
7/31/2006	1	-2.1	2.6	-2.6	1.1	-1.6	0.5
8/3/2006	2	0.6	2.8	-1.1	2.2	2.8	2.8
8/10/2006	3	0.5	2.6	0	3.1	1.5	3.6
8/17/2006	4	-1.1	1.6	-2.7	1.1	2.1	-0.5
8/24/2006	5	-3.1	0.5	-2.6	0	2.6	-2.1
Σ_{ind}		-1.0	2.0	-1.8	1.5	1.5	0.9
σ_{ind}		1.6	1.0	1.2	1.2	1.8	2.3

Patient No.8		Skull bones		C1		C4	
Date	Fraction	ΔAP (mm)	ΔSI (mm)	ΔAP (mm)	ΔSI (mm)	ΔAP (mm)	ΔSI (mm)
8/3/2006	1	-2.1	-1.6	-4.8	-1.1	-3.2	-2.1
8/21/2006	2	0	-2.5	-1	-1	3.8	-1.5
8/28/2006	3	-1	-2.6	-2.1	0	3.6	-0.5
9/4/2006	4	-1.9	-1	-1	0	3.9	-1.4
Σ_{ind}		-1.3	-1.9	-2.2	-0.5	2.0	-1.4
σ_{ind}		1.0	0.8	1.8	0.6	3.5	0.7

Patient No.9		Skull bones		C1		C4	
Date	Fraction	ΔAP (mm)	ΔSI (mm)	ΔAP (mm)	ΔSI (mm)	ΔAP (mm)	ΔSI (mm)
9/5/2006	1	-1	1.9	-2.9	1.4	-1.4	2.9
9/18/2006	2	-2.9	0	-4.8	-1.4	-1.9	-1
9/25/2006	3	-2.4	1.4	-3.9	0.5	1.4	1.9
10/2/2006	4	-1	1	-2.4	1.4	0.5	1.4
10/11/2006	5	-2.4	2.4	-2.4	2.4	1.4	2.9
10/16/2006	6	-1.4	1.4	-1.9	2.9	2.4	2.9
Σ_{ind}		-1.9	1.4	-3.1	1.2	0.4	1.8
σ_{ind}		0.8	0.8	1.1	1.5	1.7	1.5

Table II. Spreadsheets for an anterior field matched over the course of six fractions to mandible, clavicle and spinous process, respectively. ΔLR and ΔSI represent the deviations in the L-R and S-I direction of each anatomical landmark between simulation images and portal images. Positive shifts correspond to left shifts and negative shifts correspond to right shifts.

Patient No.1		Mandible		Clavicle		Spinous process	
Date	Fraction	ΔLR(mm)	ΔSI (mm)	ΔLR(mm)	ΔSI (mm)	ΔLR(mm)	ΔSI(mm)
3/1/2006	1	-0.5	2.9	-1.9	1	-2.4	3.9
3/3/2006	2	1.4	1	0.5	0.5	0.5	3.4
3/7/2006	3	1.9	0.5	3.9	1.4	0	3.9
3/14/2006	4	1	-2.9	-2.9	-1.4	-3.4	-2.4
3/21/2006	5	0	-2.9	-3.4	-1.9	-4.8	-1
3/28/2006	6	0.5	-1	-3.9	-1.9	-4.8	-1
Σ_{ind}		0.7	-0.4	-1.3	-0.4	-2.5	1.1
σ_{ind}		0.9	2.3	3.0	1.5	2.3	2.9

Patient No.2		Mandible		Clavicle		Spinous process	
Date	Fraction	ΔLR(mm)	ΔSI(mm)	ΔLR (mm)	ΔSI (mm)	ΔLR (mm)	ΔSI (mm)
4/25/2006	1	1	2.5	-1.1	3.4	-1	1.5
5/2/2006	2	-0.5	3	-3.9	1.4	-1	3
5/8/2006	3	-1.5	2.5	-2	6.5	-1.5	2.5
5/15/2006	4	-0.5	3.6	1.1	6.6	0.5	3.6
Σ_{ind}		-0.4	2.9	-1.5	4.5	-0.8	2.7
σ_{ind}		1.0	0.5	2.1	2.5	0.9	0.9

Patient No.3		Mandible		Clavicle		Spinous process	
Date	Fraction	ΔLR(mm)	ΔSI (mm)	ΔLR(mm)	ΔSI (mm)	ΔLR(mm)	ΔSI (mm)
3/8/2006	1	-2.4	-1.9	-2.3	1.9	-2.4	-1.9
3/14/2006	2	3.9	-3.9	-1.7	1	-0.5	3.9
3/20/2006	3	5.8	-0.5	-2.4	0.5	-6.8	6.3
3/27/2006	4	5.3	-4.8	-2	2	-3.4	1.4
3/28/2006	5	-4.8	-2.9	-2	2	-5.3	8.7
Σ_{ind}		1.6	-2.8	-2.1	1.5	-3.7	3.7
σ_{ind}		4.8	1.7	0.3	0.7	2.5	4.1

Patient No.4		Mandible		Clavicle		Spinous process	
Date	Fraction	ΔLR(mm)	ΔSI (mm)	ΔLR(mm)	ΔSI (mm)	ΔLR(mm)	ΔSI (mm)
3/22/2006	1	1.8	-0.5	-0.3	-1.4	1	-0.5
3/23/2006	2	0.5	-1.5	-0.5	-1.9	0.5	-1.1
3/27/2006	3	0.5	-0.5	-0.5	-1.4	0.5	-0.8
4/3/2006	4	0.3	-2.1	-1.7	-1.1	0.3	-1.8
4/10/2006	5	1.5	0.1	-1	-2	1.5	0.4
4/18/2006	6	0.5	-1	-2	-2	0	0
4/24/2006	7	-1.3	-0.3	0.5	-0.4	-1.3	-0.3
Σ_{ind}		0.6	-1.0	-0.9	-1.7	0.4	-0.7
σ_{ind}		1.0	0.8	0.9	0.6	0.9	0.7

Patient No.4		Mandible		Clavicle		Spinous process	
Date	Fraction	ΔLR(mm)	ΔSI (mm)	ΔLR(mm)	ΔSI (mm)	ΔLR(mm)	ΔSI (mm)
3/22/2006	1	1.8	-0.5	2.1	-1.8	1	-0.5
3/23/2006	2	0.5	-1.5	1	-1.1	0.5	-1.1
3/27/2006	3	0.5	-0.5	1.3	-1	0.5	-0.8
4/3/2006	4	0.3	-2.1	1.1	-2	0.3	-1.8
4/10/2006	5	1.5	0.1	2	-1	1.5	0.4
4/18/2006	6	0.5	-1	1	-2.3	0	0
Σ_{ind}		0.9	-0.9	1.4	-1.5	0.6	-0.6
σ_{ind}		0.6	0.8	0.5	0.6	0.5	0.8

Patient No.5		Mandible		Clavicle		Spinous process	
Date	Fraction	ΔLR(mm)	ΔSI (mm)	ΔLR(mm)	ΔSI (mm)	ΔLR(mm)	ΔSI (mm)
5/26/2006	1	0	0	-2	-1	-0.5	0
6/19/2006	2	-0.5	3.6	-0.5	0	-1	3.6
6/26/2006	3	0	3.9	-2.2	-3.3	-4.4	2.2
7/13/2006	4	0.5	-1.1	-0.5	-1.6	0.5	0
7/17/2006	5	0	3.9	0.6	0	1.7	2.8
Σ_{ind}		0	2.1	-0.9	-1.2	-0.7	1.7
σ_{ind}		0.4	2.4	1.2	1.4	2.3	1.6

Patient No.6		Mandible		Clavicle		Spinous process	
Date	Fraction	ΔLR (mm)	ΔSI (mm)	ΔLR (mm)	ΔSI (mm)	ΔLR (mm)	ΔSI (mm)
7/31/2006	1	0.5	-3.1	-2.5	-3.2	1.5	-3.1
8/7/2006	2	-1.5	0	-4.5	3.9	2.1	1.8
8/21/2006	3	-0.5	-2	-6.1	-1.5	3	0
8/28/2006	4	-3	-1	-5	-2	4	-1
9/4/2006	5	-2.4	-2.4	-5.8	-4.3	1.4	-1.9
Σ_{ind}		-1.4	-1.7	-4.8	-1.4	2.4	-0.8
σ_{ind}		1.4	1.2	1.4	3.2	1.1	1.9

Patient No.7		Mandible		Clavicle		Spinous process	
Date	Fraction	ΔLR (mm)	ΔSI (mm)	ΔLR (mm)	ΔSI (mm)	ΔLR (mm)	ΔSI (mm)
7/31/2006	1	0	2.1	-6.9	0.5	-6.8	1.1
8/3/2006	2	0.5	0.5	2.2	-0.5	-1.6	0.5
8/10/2006	3	-0.3	2.6	0.5	1	-3.1	3.6
8/17/2006	4	1.1	-1.1	0.5	-4.3	-2.1	0
8/24/2006	5	-0.5	-3.1	-0.5	-3.1	-3.1	-1.5
Σ_{ind}		0.2	0.2	-0.8	-1.3	-3.3	0.7
σ_{ind}		0.6	2.3	3.5	2.3	2.0	1.9

Patient No.8		Mandible		Clavicle		Spinous process	
Date	Fraction	ΔLR (mm)	ΔSI (mm)	ΔLR (mm)	ΔSI (mm)	ΔLR (mm)	ΔSI (mm)
8/3/2006	1	-0.5	-0.5	0	0.5	-0.5	0
8/21/2006	2	0	-2.5	2.5	1.5	1.5	-1
8/28/2006	3	-1.5	-2.1	4.6	1	-0.5	-0.5
9/4/2006	4	-1.4	-1.9	4.3	1	0	-2.4
Σ_{ind}		-0.9	-1.8	2.9	1.0	0.1	-1.0
σ_{ind}		0.7	0.9	2.1	0.4	0.9	1.0

Patient No.9		Mandible		Clavicle		Spinous process	
Date	Fraction	ΔLR (mm)	ΔSI (mm)	ΔLR (mm)	ΔSI (mm)	ΔLR (mm)	ΔSI (mm)
9/5/2006	1	-0.5	0	-1.9	5.3	-6.3	2.9
9/18/2006	2	-0.5	-0.7	1.9	-3.4	1	0.2
9/25/2006	3	-1	1.4	-2.9	-1	-5.3	1.4
10/2/2006	4	0	-1.5	-0.5	1.9	-3.4	0.5
10/11/2006	5	-0.5	0	-3.4	-5.8	-5.3	1.4
10/16/2006	6	-1	-1.9	-4.8	-3.4	-2.9	1.4
Σ_{ind}		-0.6	-0.5	-1.9	-1.1	-3.7	1.3
σ_{ind}		0.4	1.2	2.4	4.1	2.6	0.9

VITAE

NAME	Miss Nantaporn Naiyanet
SEX	Female
NATIONALITY	Thai
DATE OF BIRTH	26th September, 1980
PLACE OF BIRTH	Uthaithani, Thailand
INSTITUTIONS ATTENED	Naresuan University, 2003: Bachelor of Science (Radiological Technology) Chulalongkorn University, 2007: Master of Science (Medical Imaging)
HOME ADDRESS	19 Moo.4 Hattanong Meuang Uthaithani, 61000 Thailand